

High excess yield of a variety of silicon-boron radicals and their reactivity

Mohd Nazish, Yi Ding, Christina M. Legendre, Arun Kumar, Nico Graw, Brigitte Schwederski, Regine Herbst-Irmer, Parameswaran Parvathy, Pattiyl Parameswaran*, Dietmar Stalke,* Wolfgang Kaim,* and Herbert W. Roesky*

Supporting Information

Table of Contents:	Page No.
Spectra	S2-S8
X-ray crystallographic analysis	S9-S24
Computational Details	S25-S33
Cyclic voltammetry	S34-S34
References	S35

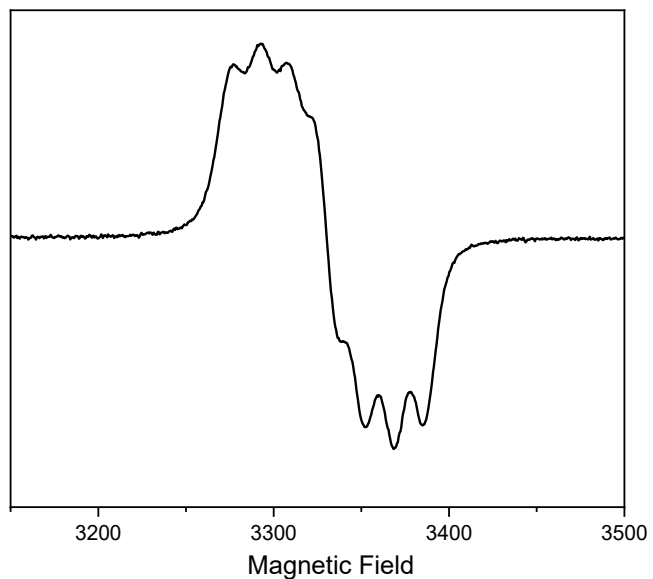


Figure S1: EPR spectrum of **2** in toluene at room temperature.

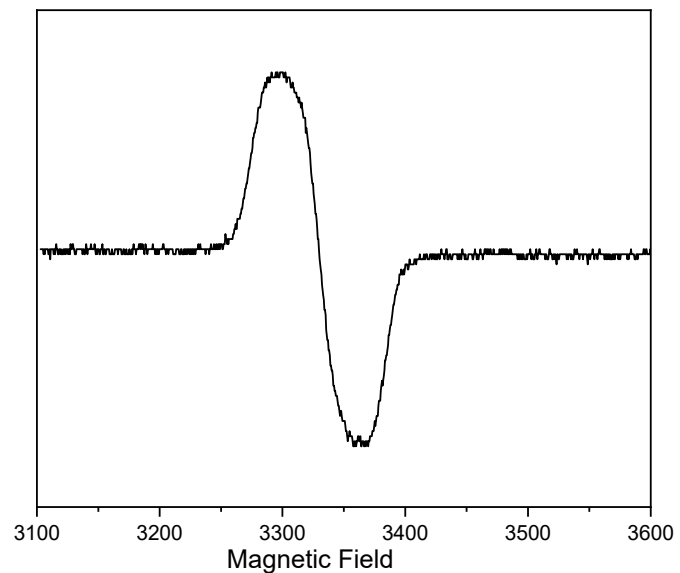


Figure S2: EPR spectrum of **3** in toluene at room temperature.

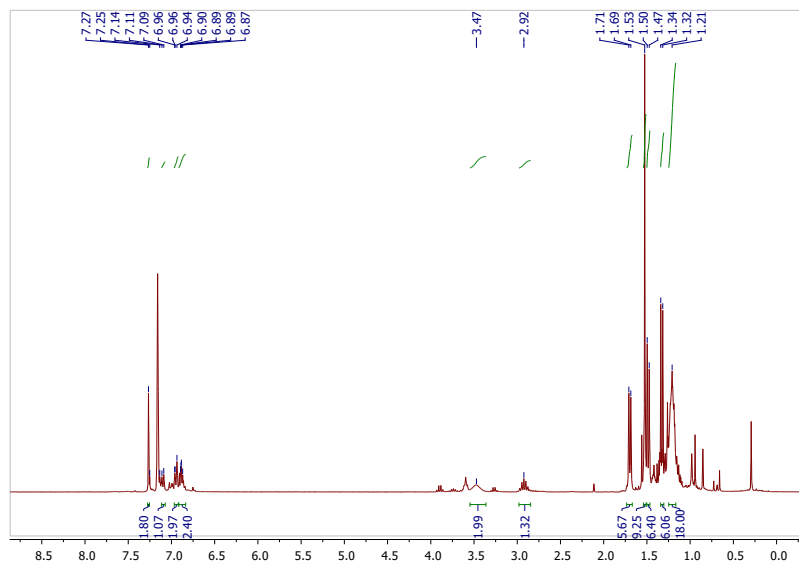


Figure S3: ^1H NMR spectrum of **4** at 298 K.

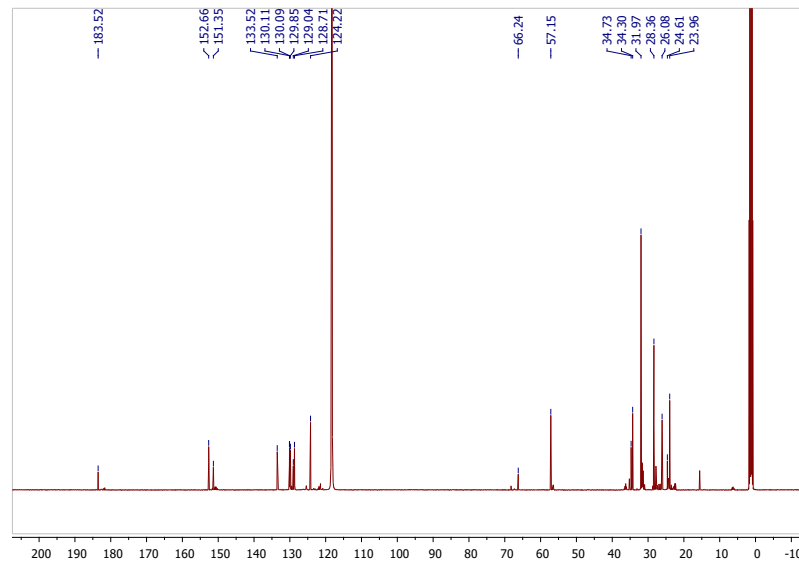


Figure S4: ^{13}C NMR spectrum of **4** at 298 K.

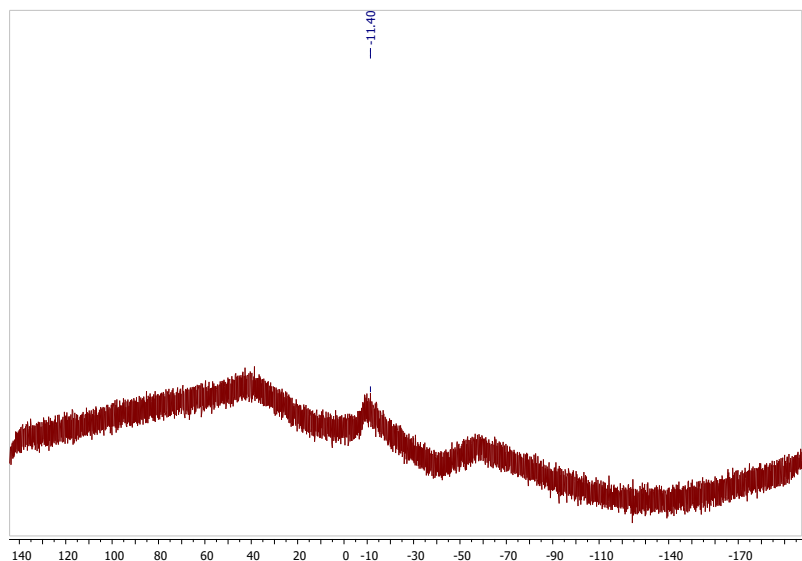


Figure S5: ^{11}B NMR spectrum of **4** at 298 K.

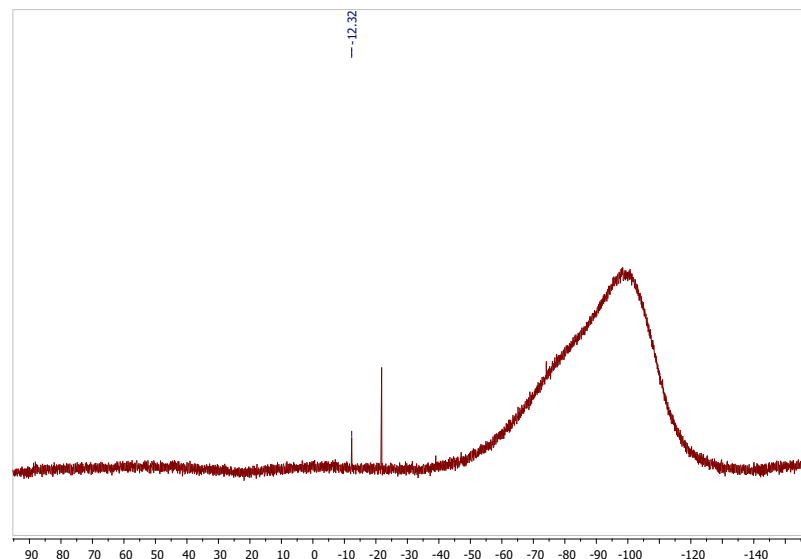


Figure S6: ^{29}Si NMR spectrum of **4** at 298 K.

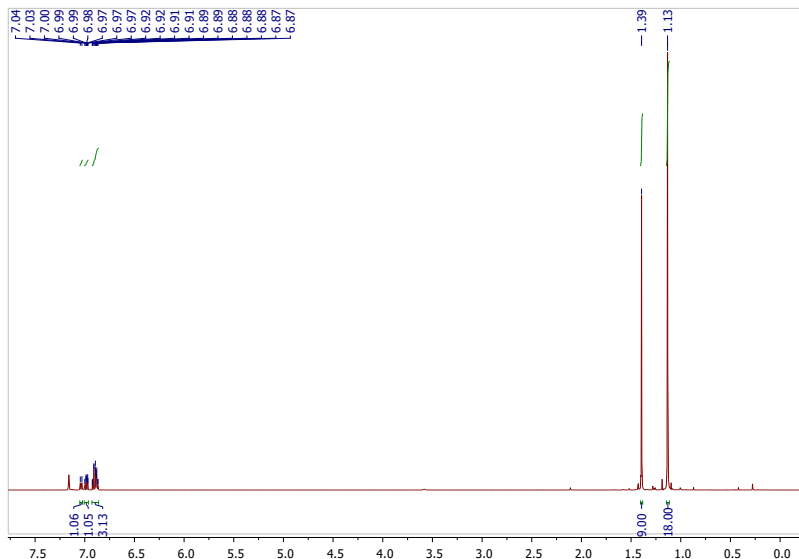


Figure S7: ¹H NMR spectrum of **5** at 298 K.

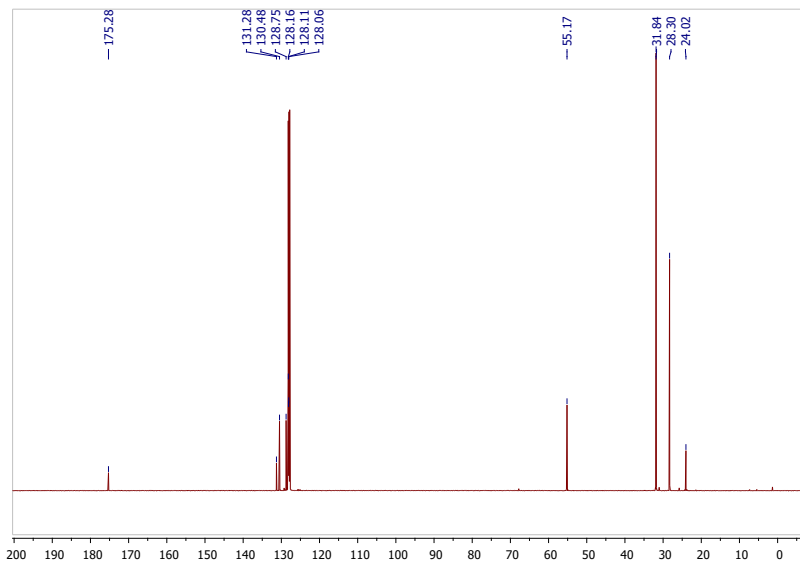


Figure S8: ¹³C NMR spectrum of **5** at 298 K.

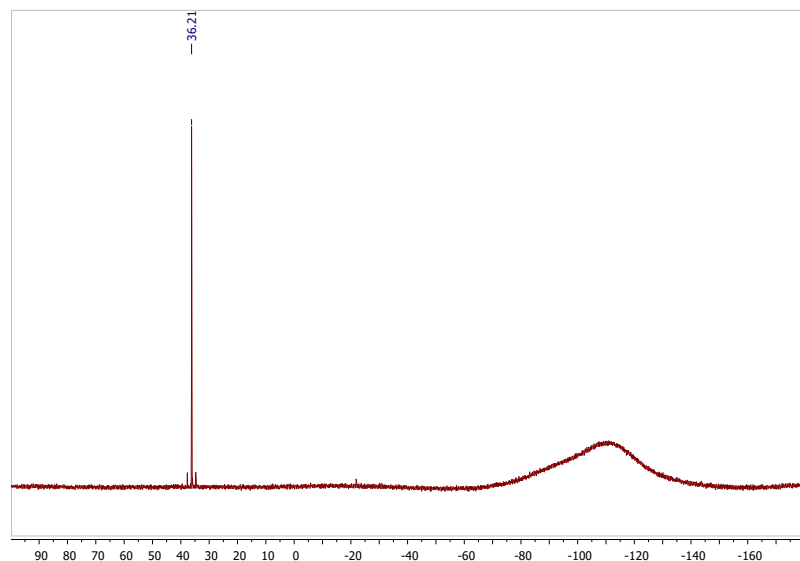


Figure S9: ^{29}Si NMR spectrum of **5** at 298 K.

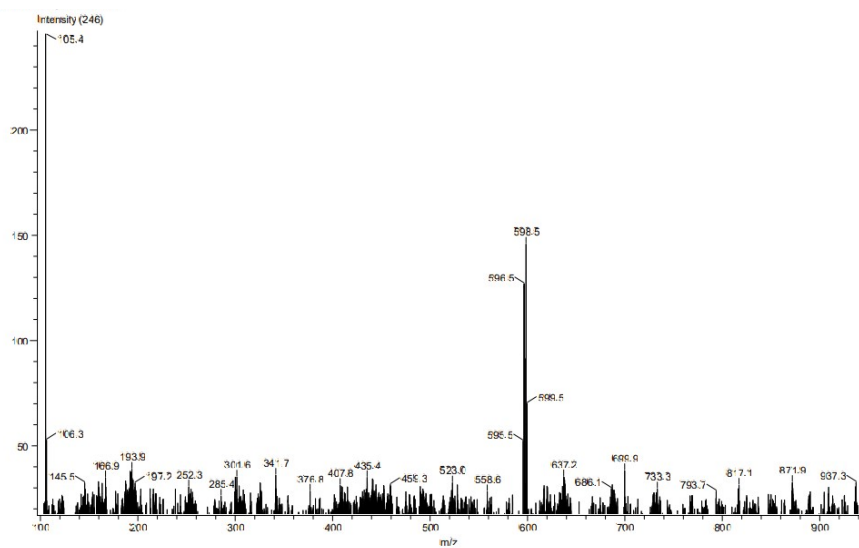


Figure S10: LIFDI mass spectrum of **1**.

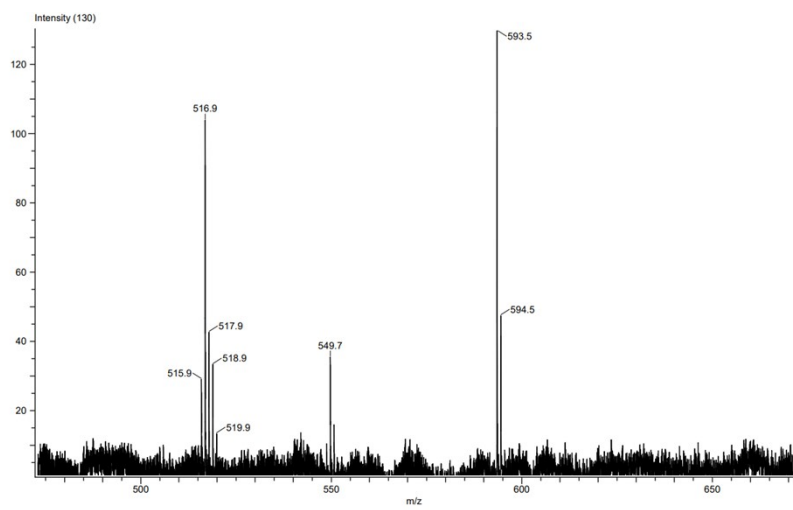


Figure S11: LIFDI mass spectrum of **2**.

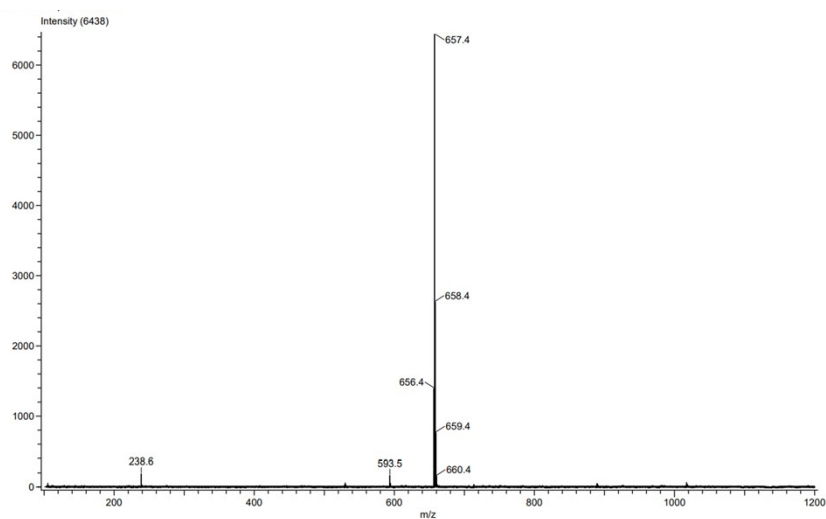


Figure S12: LIFDI mass spectrum of **3**.

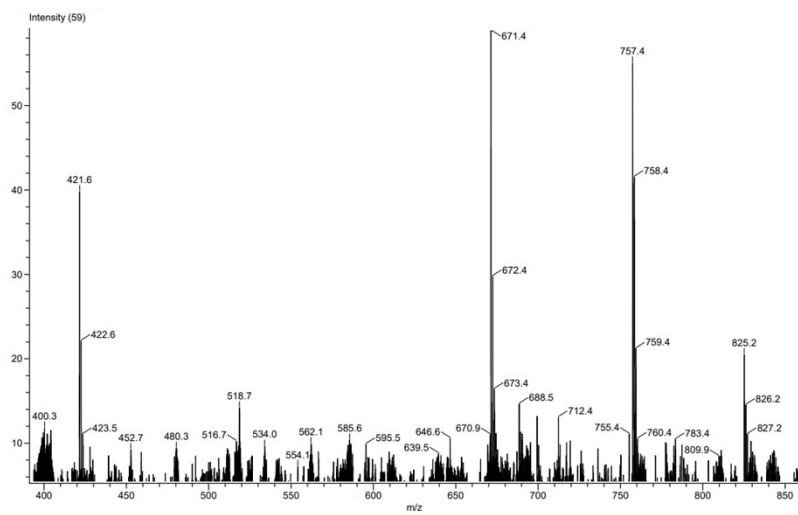


Figure S13: LIFDI mass spectrum of **4**.

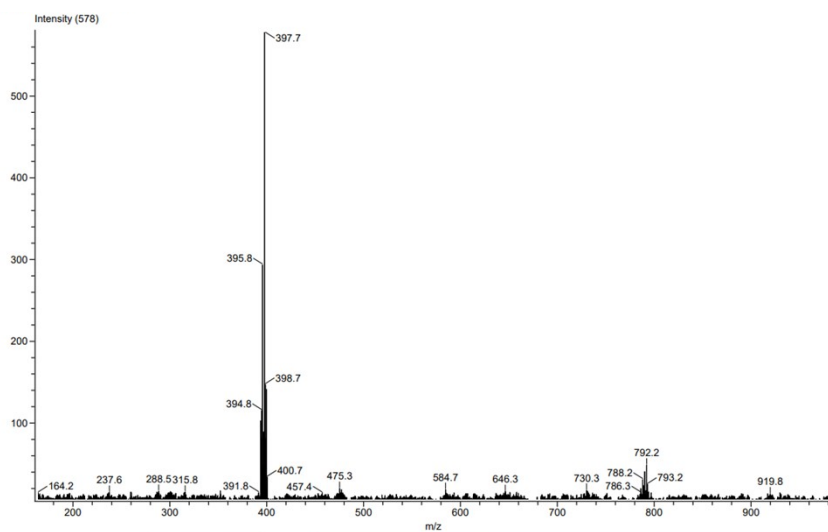


Figure S14: LIFDI mass spectrum of **5**.

Crystal Structure Determination

Crystals suitable for single crystal X-ray diffraction were mounted at low temperature in inert oil under an nitrogen atmosphere by applying the X-Temp 2 device.²² Diffraction data were collected at 100 K with a Bruker D8 three circle diffractometer equipped with an incoated Mo Microsource (**1**, **3-5**) or a Bruker Mo rotating anode (**2**) with mirror optics (MoK α radiation, $\lambda = 0.71073 \text{ \AA}$). The data were integrated with SAINT²³ and an empirical absorption correction was applied with SADABS²⁴ (**1-2**, **4-5**) or TWINABS (**3**).²⁵ The structures were solved by SHELXT²⁶ and refined on F² using SHELXL²⁷ in the graphical userinterface ShelXle.²⁸

Crystal data for **1** at 100(2) K: C₃₂H₅₂BBrN₃Si, M_r = 597.57 g/mol, 0.359 x 0.337 x 0.201 mm, monoclinic, P2₁/n, $a = 11.102(2) \text{ \AA}$, $b = 14.901(2) \text{ \AA}$, $c = 21.157(3) \text{ \AA}$, $\beta = 102.55(2)$, V = 3416.4(9) \AA^3 , Z = 4, $\mu(\text{Mo K}\alpha) = 1.262 \text{ mm}^{-1}$, $\vartheta_{\max} = 28.413^\circ$, 133144 reflections measured, 8563 independent ($R_{\text{int}} = 0.0498$), $R1 = 0.0325$ [$|I| > 2\sigma(I)$], $wR2 = 0.0830$ (all data), res. density peaks: 0.402 to - 0.335 e \AA^3 , CCDC: 2113990

Crystal data for **2** at 100(2) K: C₃₂H₅₂BiN₃Si, M_r = 644.56g/mol, 0.426 x 0.224 x 0.122 mm, monoclinic, P2₁/n, $a = 12.626(2) \text{ \AA}$, $b = 18.594(3) \text{ \AA}$, $c = 14.454(2) \text{ \AA}$, $\beta = 90.75(2)$, V = 3393.0(9) \AA^3 , Z = 4, $\mu(\text{Mo K}\alpha) = 1.003 \text{ mm}^{-1}$, $\vartheta_{\max} = 25.171^\circ$, 126965 reflections measured, 6038 independent ($R_{\text{int}} = 0.0597$), $R1 = 0.0447$ [$|I| > 2\sigma(I)$], $wR2 = 0.0938$ (all data), res. density peaks: 0.656 to – 1.317 e \AA^3 , CCDC: 2113991

Crystal data for **3** at 100(2) K: C₃₄H₅₅BiN₂Si, M_r = 657.60 g/mol, 0.255 x 0.146 x 0.125 mm, monoclinic, P2₁/n, $a = 12.623(2) \text{ \AA}$, $b = 19.291(3) \text{ \AA}$, $c = 14.451(2) \text{ \AA}$, $\beta = 92.06(2)$, V = 3516.7(9) \AA^3 , Z = 4, $\mu(\text{Mo K}\alpha) = 0.968 \text{ mm}^{-1}$, $\vartheta_{\max} = 29.284^\circ$, 70008 reflections measured, 9573 independent ($R_{\text{int}} = 0.0727$), $R1 = 0.0392$ [$|I| > 2\sigma(I)$], $wR2 = 0.0733$ (all data), res. density peaks: 0.490 to - 0.832 e \AA^3 , CCDC: 2113992

Crystal data for **4** at 100(2) K: C₃₄H₅₅BBr₂N₂Si, M_r = 690.52g/mol, 0.276 x 0.231 x 0.127 mm, monoclinic, P2₁/n, $a = 16.079(2) \text{ \AA}$, $b = 12.497(2) \text{ \AA}$, $c = 17.886(3) \text{ \AA}$, $\beta = 106.12(2)$, V = 3452.7(11) \AA^3 , Z = 4, $\mu(\text{Mo K}\alpha) = 2.408 \text{ mm}^{-1}$, $\vartheta_{\max} = 27.614^\circ$, 147210 reflections measured, 7978 independent ($R_{\text{int}} = 0.0832$), $R1 = 0.0448$ [$|I| > 2\sigma(I)$], $wR2 = 0.1226$ (all data), res. density peaks: 2.088 to – 1.235 e \AA^3 , CCDC: 2113993

Crystal data for **5** at 100(2) K: C₄₁H₆₅BrSeSi, M_r = 800.93 g/mol, 0.350 x 0.236 x 0.122mm, monoclinic, C2/c, $a = 30.532(3) \text{ \AA}$, $b = 8.760(2) \text{ \AA}$, $c = 18.768(2) \text{ \AA}$, $\beta = 122.67(2)$, V = 4225.2(14) \AA^3 , Z = 4, $\mu(\text{Mo K}\alpha) = 1.894 \text{ mm}^{-1}$, $\vartheta_{\max} = 28.421^\circ$, 64030 reflections measured,

5315 independent ($R_{\text{int}} = 0.0409$), $R1 = 0.0234$ [$I > 2\sigma I$]), $wR2 = 0.0544$ (all data), res. density peaks: 0.354 to - 0.331 e \AA^3 , CCDC: 2113994

X-ray crystallographic details

The data were collected from shock-cooled crystals at 100(2) K, on a Bruker D8 three circle diffractometer equipped with an Incoatec Mo Microsource (**1, 3, 4, 5**) or a Bruker Mo rotating anode (**2**) with mirror optics (MoK α radiation, $\lambda = 0.71073 \text{ \AA}$). The data were integrated with SAINT.¹ An empirical absorption correction was applied using SADABS² (**1, 2, 4, 5**) or TWINABS (**3**).³ The structures were solved by SHELXT⁴ and refined on F² using SHELXL⁵ in the graphical user interface SHELXLE.⁶ All non-hydrogen-atoms were refined with anisotropic displacement parameters. The hydrogen atoms were refined isotropically on calculated positions using a riding model with their U_{iso} values constrained to 1.5 U_{eq} of their pivot atoms for terminal sp³ carbon atoms and 1.2 times for all other carbon atoms.

Table S1: Crystal data for compounds **1-5**.

Compound	1	2	3	4	5
CCDC	2113990	2113991	2113992	2113993	2113994
Empirical formula	C ₃₂ H ₅₂ BBrN ₃ Si	C ₃₂ H ₅₂ BIN ₃ Si	C ₃₄ H ₅₅ BIN ₂ Si	C ₃₄ H ₅₅ BBr ₂ N ₂ Si	C ₄₁ H ₆₅ BrN ₄ SeSi
Formula weight (g/mol)	597.57	644.56	657.60	690.52	800.93
Temperature (K)	100(2)	100(2)	100(2)	100(2)	100(2)
Wavelength (Å)	0.71073	0.71073	0.71073	0.71073	0.71073
Crystal system	Monoclinic	Monoclinic	Monoclinic	Monoclinic	Monoclinic
Space group	P2 ₁ /n	P2 ₁ /n	P2 ₁ /n	P2 ₁ /n	C2/c
a (Å)	11.102(2)	12.626(2)	12.623(2)	16.079(3)	30.532(3)
b (Å)	14.901(2)	18.594(3)	19.291(3)	12.497(2)	8.760(2)
c (Å)	21.157(3)	14.454(2)	14.451(2)	17.886(3)	18.768(2)
β (deg)	102.55(2)	90.75(2)	92.06(2)	106.12(2)	122.67(2)
V (Å ³)	3416.4(9)	3393.0(9)	3516.7(9)	3452.7(11)	4225.2(14)
Z	4	4	4	4	4
Density (Mg/m ³)	1.162	1.262	1.242	1.328	1.259

μ/mm^{-1}	1.262	1.003	0.968	2.408	1.894
Crystal size(mm)	0.359 x 0.337 x 0.201	0.426 x 0.224 x 0.122	0.255 x 0.146 x 0.125	0.276 x 0.231 x 0.127	0.350 x 0.236 x 0.122
Crystal color, shape	red blocks	orange plates	red blocks	colourless blocks	colourless blocks
Θ range (deg)	1.685 to 28.413	1.095 to 25.171	1.761 to 29.284	1.508 to 27.614	1.585 to 28.421
Reflections collected	133144	126965	70008	147210	64030
Independent reflections	8563	6038	9573	7978	5315
R_{int}	0.0498	0.0597	0.0727	0.0832	0.0409
Data/restraints/parameters	8563/175/389	6038/0/358	9573/0/368	7978/0/376	5315/117/295
$R1 (I > 2\sigma(I))$	0.0325	0.0447	0.0392	0.0448	0.0234
$wR2$ (all data)	0.0830	0.0938	0.0733	0.1226	0.0544
$\Delta\rho_{\text{max}}/\Delta\rho_{\text{min}}(\text{e \AA}^{-3})$	0.402 / -0.335	0.656 / -1.317	0.490 / -0.832	2.088/-1.235	0.354 / -0.333

Crystal structure of **1**

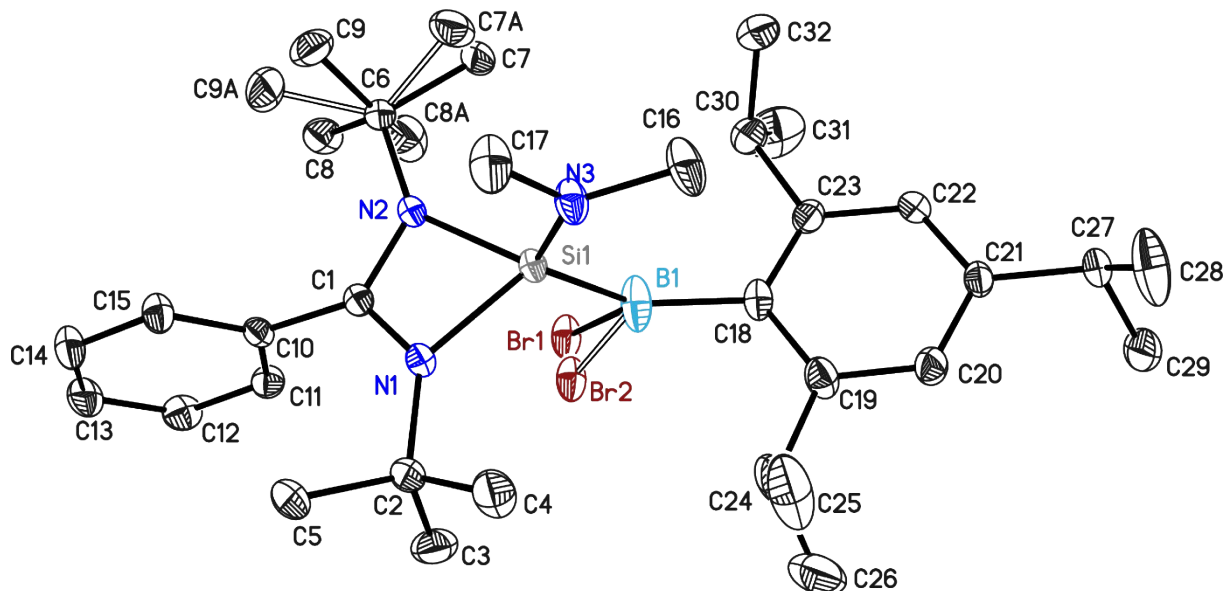


Figure S15: Crystal structure of **1**. The anisotropic displacement parameters are depicted at the 50% probability level. Hydrogen atoms are omitted for clarity.

One t-butyl group and the Si-Br moiety were disordered over two positions. They were refined with distance restraints and restraints for the anisotropic displacement parameters. The occupancies of the minor components refined to 0.116(3) and 0.0706(10) respectively.

Table S2: Bond lengths [Å] and angles [°] for **1**.

Br(1)-B(1)	2.0247(19)	N(2)-C(6)	1.4815(19)
Br(2)-B(1)	1.921(3)	C(6)-C(9A)	1.515(10)
B(1)-C(18)	1.590(2)	C(6)-C(7)	1.526(2)
B(1)-Si(1)	1.9292(19)	C(6)-C(8)	1.527(2)
Si(1)-N(3)	1.6946(13)	C(6)-C(7A)	1.535(10)
Si(1)-N(2)	1.8407(13)	C(6)-C(9)	1.538(2)
Si(1)-N(1)	1.8475(12)	C(6)-C(8A)	1.554(11)
Si(1)-C(1)	2.2984(14)	C(10)-C(15)	1.391(2)
N(1)-C(1)	1.3387(19)	C(10)-C(11)	1.395(2)
N(1)-C(2)	1.4829(19)	C(11)-C(12)	1.391(2)
C(1)-N(2)	1.3394(18)	C(12)-C(13)	1.387(2)
C(1)-C(10)	1.4908(19)	C(13)-C(14)	1.385(2)
C(2)-C(5)	1.530(2)	C(14)-C(15)	1.392(2)
C(2)-C(3)	1.530(2)	C(18)-C(23)	1.410(2)
C(2)-C(4)	1.533(2)	C(18)-C(19)	1.413(2)
N(3)-C(16)	1.4513(19)	C(19)-C(20)	1.399(2)
N(3)-C(17)	1.454(2)	C(19)-C(24)	1.517(2)

C(20)-C(21)	1.387(2)	N(1)-C(2)-C(4)	105.00(12)
C(21)-C(22)	1.388(2)	C(5)-C(2)-C(4)	108.91(14)
C(21)-C(27)	1.520(2)	C(3)-C(2)-C(4)	109.62(14)
C(22)-C(23)	1.397(2)	C(16)-N(3)-C(17)	112.92(13)
C(23)-C(30)	1.523(2)	C(16)-N(3)-Si(1)	124.09(11)
C(24)-C(26)	1.519(4)	C(17)-N(3)-Si(1)	122.83(11)
C(24)-C(25)	1.532(3)	C(1)-N(2)-C(6)	131.21(12)
C(27)-C(29)	1.518(2)	C(1)-N(2)-Si(1)	91.17(9)
C(27)-C(28)	1.529(3)	C(6)-N(2)-Si(1)	137.62(9)
C(30)-C(31)	1.513(3)	N(2)-C(6)-C(9A)	113.5(6)
C(30)-C(32)	1.524(3)	N(2)-C(6)-C(7)	106.60(12)
		N(2)-C(6)-C(8)	112.99(12)
C(18)-B(1)-Br(2)	118.56(15)	C(7)-C(6)-C(8)	108.90(14)
C(18)-B(1)-Si(1)	131.30(12)	N(2)-C(6)-C(7A)	105.7(6)
Br(2)-B(1)-Si(1)	108.74(12)	C(9A)-C(6)-C(7A)	113.7(9)
C(18)-B(1)-Br(1)	118.92(12)	N(2)-C(6)-C(9)	107.69(13)
Si(1)-B(1)-Br(1)	109.47(9)	C(7)-C(6)-C(9)	109.96(14)
N(3)-Si(1)-N(2)	112.98(6)	C(8)-C(6)-C(9)	110.60(14)
N(3)-Si(1)-N(1)	110.59(6)	N(2)-C(6)-C(8A)	103.0(6)
N(2)-Si(1)-N(1)	70.86(6)	C(9A)-C(6)-C(8A)	111.1(9)
N(3)-Si(1)-B(1)	119.56(7)	C(7A)-C(6)-C(8A)	109.2(9)
N(2)-Si(1)-B(1)	114.81(7)	C(15)-C(10)-C(11)	120.28(13)
N(1)-Si(1)-B(1)	118.41(8)	C(15)-C(10)-C(1)	122.33(13)
N(3)-Si(1)-C(1)	121.10(6)	C(11)-C(10)-C(1)	117.38(12)
N(2)-Si(1)-C(1)	35.64(5)	C(12)-C(11)-C(10)	119.43(14)
N(1)-Si(1)-C(1)	35.62(5)	C(13)-C(12)-C(11)	120.40(14)
B(1)-Si(1)-C(1)	119.33(7)	C(14)-C(13)-C(12)	119.97(14)
C(1)-N(1)-C(2)	130.50(12)	C(13)-C(14)-C(15)	120.33(15)
C(1)-N(1)-Si(1)	90.89(9)	C(10)-C(15)-C(14)	119.59(14)
C(2)-N(1)-Si(1)	136.13(10)	C(23)-C(18)-C(19)	117.05(13)
N(1)-C(1)-N(2)	105.95(12)	C(23)-C(18)-B(1)	120.64(15)
N(1)-C(1)-C(10)	126.56(12)	C(19)-C(18)-B(1)	122.18(14)
N(2)-C(1)-C(10)	127.22(13)	C(20)-C(19)-C(18)	120.71(14)
N(1)-C(1)-Si(1)	53.49(7)	C(20)-C(19)-C(24)	117.73(15)
N(2)-C(1)-Si(1)	53.20(7)	C(18)-C(19)-C(24)	121.55(14)
C(10)-C(1)-Si(1)	167.93(10)	C(21)-C(20)-C(19)	121.94(15)
N(1)-C(2)-C(5)	111.53(12)	C(20)-C(21)-C(22)	117.36(14)
N(1)-C(2)-C(3)	110.22(13)	C(20)-C(21)-C(27)	121.03(14)
C(5)-C(2)-C(3)	111.34(13)	C(22)-C(21)-C(27)	121.60(14)

C(21)-C(22)-C(23)	122.20(14)	C(29)-C(27)-C(21)	110.77(14)
C(22)-C(23)-C(18)	120.61(14)	C(29)-C(27)-C(28)	111.44(18)
C(22)-C(23)-C(30)	118.60(14)	C(21)-C(27)-C(28)	111.50(15)
C(18)-C(23)-C(30)	120.76(14)	C(31)-C(30)-C(23)	112.35(16)
C(19)-C(24)-C(26)	112.58(18)	C(31)-C(30)-C(32)	112.03(18)
C(19)-C(24)-C(25)	110.79(18)	C(23)-C(30)-C(32)	111.83(15)
C(26)-C(24)-C(25)	111.6(2)		

Crystal structure of **2**

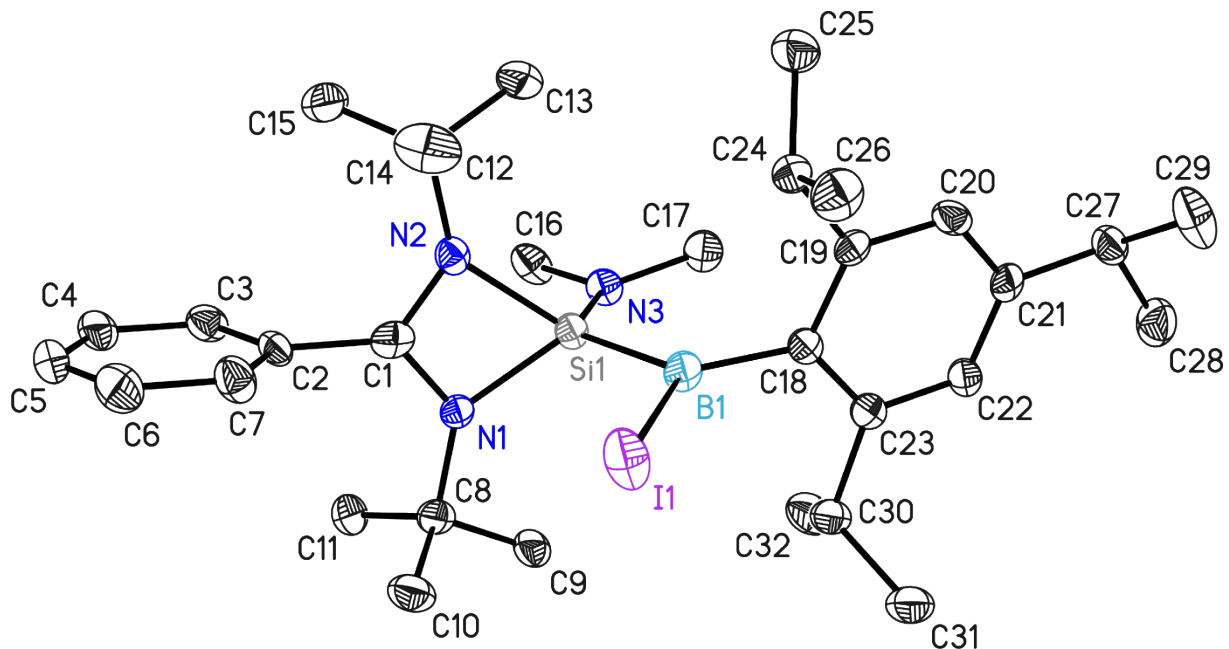


Figure S16: Crystal structure of **2**. The anisotropic displacement parameters are depicted at the 50% probability level. Hydrogen atoms are omitted for clarity.

The structure was refined as a pseudo-merohedral twin with the twin law $(-1\ 0\ 0\ 0\ -1\ 0\ 0\ 0\ 1)$. The occupancy of the minor component refined to 0.2999(17).

Table S3: Bond lengths [\AA] and angles [$^\circ$] for **2**.

I(1)-B(1)	2.221(5)	N(2)-C(12)	1.501(7)
Si(1)-N(3)	1.700(3)	N(3)-C(16)	1.452(6)
Si(1)-N(1)	1.818(4)	N(3)-C(17)	1.474(6)
Si(1)-N(2)	1.877(5)	C(1)-C(2)	1.497(6)
Si(1)-B(1)	1.930(5)	C(2)-C(7)	1.386(6)
Si(1)-C(1)	2.312(4)	C(2)-C(3)	1.390(6)
N(1)-C(1)	1.352(7)	C(3)-C(4)	1.394(7)
N(1)-C(8)	1.487(6)	C(4)-C(5)	1.380(7)
N(2)-C(1)	1.327(7)	C(5)-C(6)	1.389(7)

C(6)-C(7)	1.390(6)	C(12)-N(2)-Si(1)	136.9(3)
C(8)-C(10)	1.525(7)	C(16)-N(3)-C(17)	112.3(3)
C(8)-C(11)	1.534(6)	C(16)-N(3)-Si(1)	122.1(3)
C(8)-C(9)	1.540(8)	C(17)-N(3)-Si(1)	124.3(3)
C(12)-C(13)	1.514(7)	N(2)-C(1)-N(1)	105.9(4)
C(12)-C(15)	1.515(7)	N(2)-C(1)-C(2)	125.7(5)
C(12)-C(14)	1.528(8)	N(1)-C(1)-C(2)	128.5(5)
C(18)-C(19)	1.419(7)	N(2)-C(1)-Si(1)	54.3(2)
C(18)-C(23)	1.427(7)	N(1)-C(1)-Si(1)	51.8(2)
C(18)-B(1)	1.573(6)	C(2)-C(1)-Si(1)	175.6(3)
C(19)-C(20)	1.386(7)	C(7)-C(2)-C(3)	120.8(4)
C(19)-C(24)	1.547(8)	C(7)-C(2)-C(1)	119.1(4)
C(20)-C(21)	1.411(8)	C(3)-C(2)-C(1)	120.0(4)
C(21)-C(22)	1.371(7)	C(2)-C(3)-C(4)	119.2(4)
C(21)-C(27)	1.530(6)	C(5)-C(4)-C(3)	120.2(4)
C(22)-C(23)	1.394(7)	C(4)-C(5)-C(6)	120.2(4)
C(23)-C(30)	1.522(7)	C(5)-C(6)-C(7)	120.1(5)
C(24)-C(25)	1.515(7)	C(2)-C(7)-C(6)	119.4(4)
C(24)-C(26)	1.535(7)	N(1)-C(8)-C(10)	110.1(4)
C(27)-C(29)	1.520(7)	N(1)-C(8)-C(11)	110.8(4)
C(27)-C(28)	1.561(9)	C(10)-C(8)-C(11)	110.7(4)
C(30)-C(32)	1.537(7)	N(1)-C(8)-C(9)	106.0(4)
C(30)-C(31)	1.541(7)	C(10)-C(8)-C(9)	110.8(4)
		C(11)-C(8)-C(9)	108.4(4)
N(3)-Si(1)-N(1)	108.7(2)	N(2)-C(12)-C(13)	104.1(4)
N(3)-Si(1)-N(2)	108.4(2)	N(2)-C(12)-C(15)	112.5(4)
N(1)-Si(1)-N(2)	70.66(16)	C(13)-C(12)-C(15)	108.8(5)
N(3)-Si(1)-B(1)	119.2(2)	N(2)-C(12)-C(14)	109.6(4)
N(1)-Si(1)-B(1)	119.9(2)	C(13)-C(12)-C(14)	109.9(5)
N(2)-Si(1)-B(1)	120.1(2)	C(15)-C(12)-C(14)	111.7(5)
N(3)-Si(1)-C(1)	115.23(16)	C(19)-C(18)-C(23)	117.3(4)
N(1)-Si(1)-C(1)	35.8(2)	C(19)-C(18)-B(1)	120.6(5)
N(2)-Si(1)-C(1)	35.0(2)	C(23)-C(18)-B(1)	121.7(4)
B(1)-Si(1)-C(1)	125.56(18)	C(20)-C(19)-C(18)	119.6(5)
C(1)-N(1)-C(8)	130.7(4)	C(20)-C(19)-C(24)	120.5(5)
C(1)-N(1)-Si(1)	92.4(3)	C(18)-C(19)-C(24)	119.9(5)
C(8)-N(1)-Si(1)	136.4(4)	C(19)-C(20)-C(21)	122.4(5)
C(1)-N(2)-C(12)	132.0(4)	C(22)-C(21)-C(20)	118.0(4)
C(1)-N(2)-Si(1)	90.7(3)	C(22)-C(21)-C(27)	121.9(5)

C(20)-C(21)-C(27)	120.1(5)	C(29)-C(27)-C(28)	109.2(5)
C(21)-C(22)-C(23)	121.4(5)	C(21)-C(27)-C(28)	114.1(4)
C(22)-C(23)-C(18)	121.0(4)	C(23)-C(30)-C(32)	111.5(4)
C(22)-C(23)-C(30)	117.9(5)	C(23)-C(30)-C(31)	111.5(4)
C(18)-C(23)-C(30)	121.2(4)	C(32)-C(30)-C(31)	110.1(5)
C(25)-C(24)-C(26)	110.6(4)	C(18)-B(1)-Si(1)	126.4(3)
C(25)-C(24)-C(19)	114.7(4)	C(18)-B(1)-I(1)	118.9(3)
C(26)-C(24)-C(19)	110.4(4)	Si(1)-B(1)-I(1)	114.6(2)
C(29)-C(27)-C(21)	110.1(4)		

Crystal structure of **3**

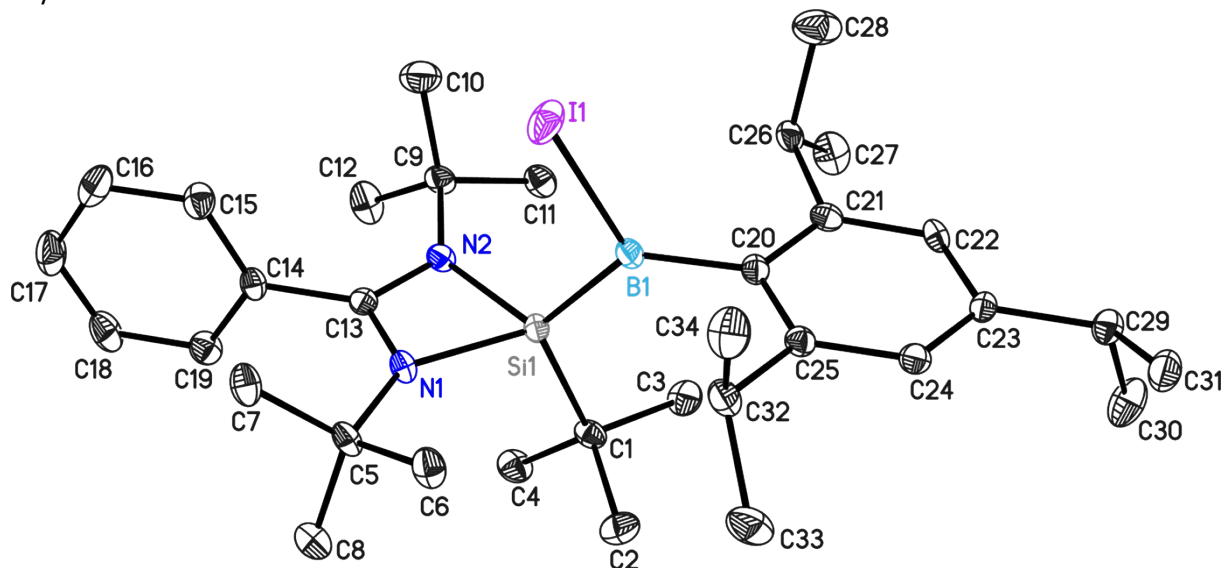


Figure S17: Crystal structure of **3**. The anisotropic displacement parameters are depicted at the 50% probability level. Hydrogen atoms are omitted for clarity. The structure was refined as a non-merohedral twin. The occupancy of the minor component refined to 0.4351(8).

Table S4: Bond lengths [Å] and angles [°] for **3**

I(1)-B(1)	2.227(2)	N(1)-C(5)	1.479(4)
Si(1)-N(1)	1.852(3)	C(1)-C(3)	1.536(4)
Si(1)-N(2)	1.854(2)	C(1)-C(2)	1.539(4)
Si(1)-C(1)	1.906(2)	C(1)-C(4)	1.542(3)
Si(1)-B(1)	1.916(3)	B(1)-C(20)	1.590(3)
Si(1)-C(13)	2.303(2)	N(2)-C(13)	1.331(4)
N(1)-C(13)	1.342(3)	N(2)-C(9)	1.486(3)

C(5)-C(6)	1.525(4)	C(13)-N(1)-C(5)	129.3(2)
C(5)-C(7)	1.530(4)	C(13)-N(1)-Si(1)	90.83(16)
C(5)-C(8)	1.538(4)	C(5)-N(1)-Si(1)	139.82(18)
C(9)-C(11)	1.526(4)	C(3)-C(1)-C(2)	107.2(2)
C(9)-C(10)	1.527(4)	C(3)-C(1)-C(4)	109.8(2)
C(9)-C(12)	1.531(4)	C(2)-C(1)-C(4)	109.0(2)
C(13)-C(14)	1.488(3)	C(3)-C(1)-Si(1)	110.17(17)
C(14)-C(19)	1.390(3)	C(2)-C(1)-Si(1)	108.95(18)
C(14)-C(15)	1.392(3)	C(4)-C(1)-Si(1)	111.64(17)
C(15)-C(16)	1.390(3)	C(20)-B(1)-Si(1)	129.63(17)
C(16)-C(17)	1.380(4)	C(20)-B(1)-I(1)	117.52(15)
C(17)-C(18)	1.378(4)	Si(1)-B(1)-I(1)	112.83(11)
C(18)-C(19)	1.390(3)	C(13)-N(2)-C(9)	129.7(2)
C(20)-C(21)	1.409(4)	C(13)-N(2)-Si(1)	91.12(15)
C(20)-C(25)	1.417(4)	C(9)-N(2)-Si(1)	138.8(2)
C(21)-C(22)	1.403(4)	N(1)-C(5)-C(6)	106.9(2)
C(21)-C(26)	1.515(4)	N(1)-C(5)-C(7)	112.3(2)
C(22)-C(23)	1.393(4)	C(6)-C(5)-C(7)	107.8(2)
C(23)-C(24)	1.378(4)	N(1)-C(5)-C(8)	110.0(2)
C(23)-C(29)	1.530(3)	C(6)-C(5)-C(8)	110.0(2)
C(24)-C(25)	1.392(4)	C(7)-C(5)-C(8)	109.7(2)
C(25)-C(32)	1.518(4)	N(2)-C(9)-C(11)	106.2(2)
C(26)-C(28)	1.519(4)	N(2)-C(9)-C(10)	109.6(2)
C(26)-C(27)	1.526(4)	C(11)-C(9)-C(10)	109.5(2)
C(29)-C(31)	1.513(4)	N(2)-C(9)-C(12)	111.8(2)
C(29)-C(30)	1.530(3)	C(11)-C(9)-C(12)	108.5(2)
C(32)-C(33)	1.525(4)	C(10)-C(9)-C(12)	111.1(2)
C(32)-C(34)	1.532(4)	N(2)-C(13)-N(1)	107.13(19)
		N(2)-C(13)-C(14)	126.2(2)
N(1)-Si(1)-N(2)	70.92(10)	N(1)-C(13)-C(14)	126.6(3)
N(1)-Si(1)-C(1)	108.66(11)	N(2)-C(13)-Si(1)	53.60(12)
N(2)-Si(1)-C(1)	109.12(12)	N(1)-C(13)-Si(1)	53.54(13)
N(1)-Si(1)-B(1)	119.52(12)	C(14)-C(13)-Si(1)	179.8(2)
N(2)-Si(1)-B(1)	120.36(12)	C(19)-C(14)-C(15)	120.3(2)
C(1)-Si(1)-B(1)	118.78(11)	C(19)-C(14)-C(13)	119.7(2)
N(1)-Si(1)-C(13)	35.63(10)	C(15)-C(14)-C(13)	120.0(2)
N(2)-Si(1)-C(13)	35.29(10)	C(16)-C(15)-C(14)	119.5(2)
C(1)-Si(1)-C(13)	113.67(10)	C(17)-C(16)-C(15)	120.0(2)
B(1)-Si(1)-C(13)	127.54(9)	C(18)-C(17)-C(16)	120.7(2)

C(17)-C(18)-C(19)	120.0(2)	C(24)-C(25)-C(20)	120.3(3)
C(14)-C(19)-C(18)	119.5(2)	C(24)-C(25)-C(32)	119.1(2)
C(21)-C(20)-C(25)	117.5(2)	C(20)-C(25)-C(32)	120.5(2)
C(21)-C(20)-B(1)	121.4(2)	C(21)-C(26)-C(28)	109.7(2)
C(25)-C(20)-B(1)	121.2(3)	C(21)-C(26)-C(27)	113.5(2)
C(22)-C(21)-C(20)	120.6(2)	C(28)-C(26)-C(27)	110.3(3)
C(22)-C(21)-C(26)	117.4(2)	C(31)-C(29)-C(23)	113.4(2)
C(20)-C(21)-C(26)	121.8(2)	C(31)-C(29)-C(30)	111.1(2)
C(23)-C(22)-C(21)	121.3(2)	C(23)-C(29)-C(30)	109.6(2)
C(24)-C(23)-C(22)	118.0(2)	C(25)-C(32)-C(33)	114.1(2)
C(24)-C(23)-C(29)	123.4(2)	C(25)-C(32)-C(34)	110.4(2)
C(22)-C(23)-C(29)	118.6(2)	C(33)-C(32)-C(34)	110.2(2)
C(23)-C(24)-C(25)	122.3(2)		

Crystal structure of **4**

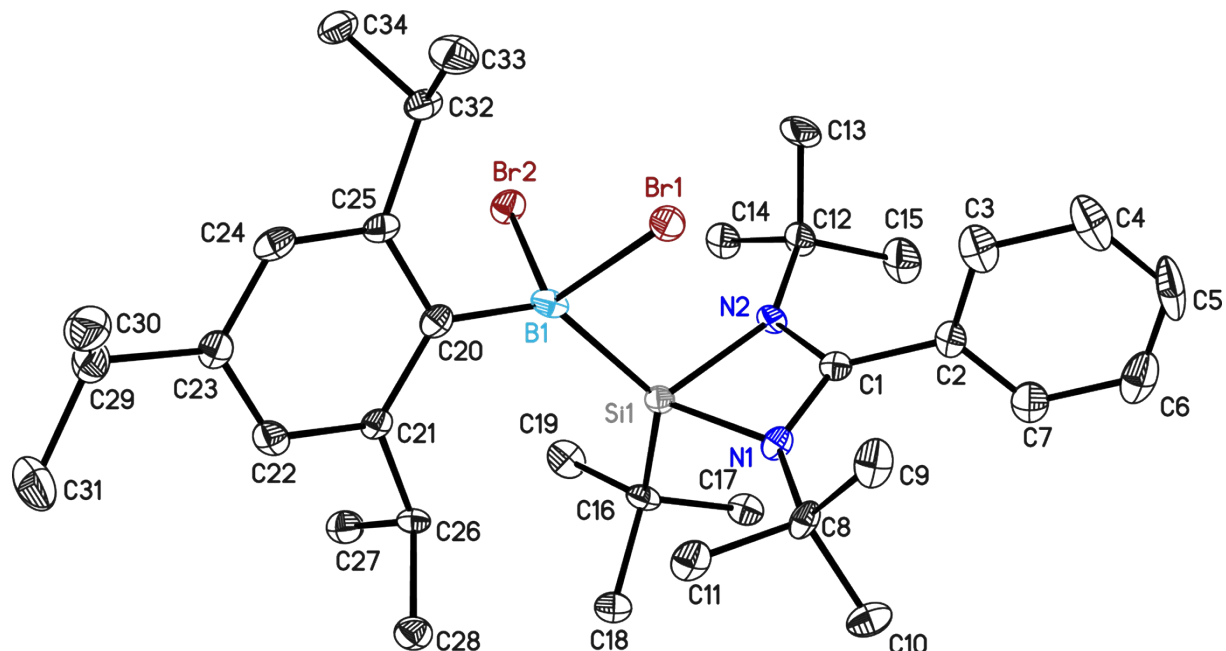


Figure S18: Crystal structure of **4**. The anisotropic displacement parameters are depicted at the 50% probability level. Hydrogen atoms are omitted for clarity.

Table S5: Bond lengths [Å] and angles [°] for **4**

Br(1)-B(1)	2.106(4)	Si(1)-B(1)	2.096(4)
Si(1)-N(1)	1.826(3)	Si(1)-C(1)	2.279(3)
Si(1)-N(2)	1.847(3)	N(1)-C(1)	1.341(4)
Si(1)-C(16)	1.930(3)	N(1)-C(8)	1.493(4)

C(1)-N(2)	1.336(4)	N(1)-Si(1)-B(1)	113.87(13)
C(1)-C(2)	1.487(4)	N(2)-Si(1)-B(1)	109.28(13)
B(1)-C(20)	1.627(5)	C(16)-Si(1)-B(1)	133.22(14)
B(1)-Br(2)	2.090(3)	N(1)-Si(1)-C(1)	36.04(11)
N(2)-C(12)	1.499(4)	N(2)-Si(1)-C(1)	35.89(11)
C(2)-C(3)	1.385(5)	C(16)-Si(1)-C(1)	111.29(13)
C(2)-C(7)	1.391(5)	B(1)-Si(1)-C(1)	115.20(13)
C(3)-C(4)	1.392(5)	C(1)-N(1)-C(8)	130.2(3)
C(4)-C(5)	1.375(7)	C(1)-N(1)-Si(1)	90.75(19)
C(5)-C(6)	1.380(7)	C(8)-N(1)-Si(1)	137.8(2)
C(6)-C(7)	1.385(5)	N(2)-C(1)-N(1)	107.2(3)
C(8)-C(11)	1.525(5)	N(2)-C(1)-C(2)	126.9(3)
C(8)-C(9)	1.527(4)	N(1)-C(1)-C(2)	125.9(3)
C(8)-C(10)	1.534(5)	N(2)-C(1)-Si(1)	54.12(15)
C(12)-C(13)	1.527(5)	N(1)-C(1)-Si(1)	53.21(15)
C(12)-C(14)	1.529(5)	C(2)-C(1)-Si(1)	175.6(2)
C(12)-C(15)	1.532(5)	C(20)-B(1)-Br(2)	104.8(2)
C(16)-C(19)	1.538(4)	C(20)-B(1)-Si(1)	137.0(2)
C(16)-C(18)	1.546(4)	Br(2)-B(1)-Si(1)	98.95(15)
C(16)-C(17)	1.549(4)	C(20)-B(1)-Br(1)	107.7(2)
C(20)-C(21)	1.416(4)	Br(2)-B(1)-Br(1)	111.09(16)
C(20)-C(25)	1.434(4)	Si(1)-B(1)-Br(1)	96.11(15)
C(21)-C(22)	1.402(4)	C(1)-N(2)-C(12)	128.1(3)
C(21)-C(26)	1.513(4)	C(1)-N(2)-Si(1)	89.99(19)
C(22)-C(23)	1.374(5)	C(12)-N(2)-Si(1)	141.9(2)
C(23)-C(24)	1.398(5)	C(3)-C(2)-C(7)	120.0(3)
C(23)-C(29)	1.526(4)	C(3)-C(2)-C(1)	119.7(3)
C(24)-C(25)	1.391(5)	C(7)-C(2)-C(1)	120.4(3)
C(25)-C(32)	1.535(4)	C(2)-C(3)-C(4)	119.6(4)
C(26)-C(28)	1.526(4)	C(5)-C(4)-C(3)	120.4(4)
C(26)-C(27)	1.537(4)	C(4)-C(5)-C(6)	120.1(4)
C(29)-C(31)	1.524(5)	C(5)-C(6)-C(7)	120.3(4)
C(29)-C(30)	1.526(5)	C(6)-C(7)-C(2)	119.8(4)
C(32)-C(33)	1.534(5)	N(1)-C(8)-C(11)	105.8(2)
C(32)-C(34)	1.536(5)	N(1)-C(8)-C(9)	113.2(3)
		C(11)-C(8)-C(9)	108.7(3)
N(1)-Si(1)-N(2)	71.85(12)	N(1)-C(8)-C(10)	109.7(3)
N(1)-Si(1)-C(16)	106.37(13)	C(11)-C(8)-C(10)	109.9(3)
N(2)-Si(1)-C(16)	105.01(13)	C(9)-C(8)-C(10)	109.5(3)

N(2)-C(12)-C(13)	109.7(3)	C(23)-C(22)-C(21)	122.4(3)
N(2)-C(12)-C(14)	108.9(3)	C(22)-C(23)-C(24)	116.2(3)
C(13)-C(12)-C(14)	108.6(3)	C(22)-C(23)-C(29)	123.4(3)
N(2)-C(12)-C(15)	111.4(3)	C(24)-C(23)-C(29)	120.4(3)
C(13)-C(12)-C(15)	110.5(3)	C(25)-C(24)-C(23)	123.9(3)
C(14)-C(12)-C(15)	107.7(3)	C(24)-C(25)-C(20)	119.8(3)
C(19)-C(16)-C(18)	108.6(3)	C(24)-C(25)-C(32)	114.4(3)
C(19)-C(16)-C(17)	109.4(3)	C(20)-C(25)-C(32)	125.8(3)
C(18)-C(16)-C(17)	104.8(3)	C(21)-C(26)-C(28)	113.4(3)
C(19)-C(16)-Si(1)	110.7(2)	C(21)-C(26)-C(27)	109.4(3)
C(18)-C(16)-Si(1)	114.2(2)	C(28)-C(26)-C(27)	110.7(3)
C(17)-C(16)-Si(1)	108.9(2)	C(31)-C(29)-C(23)	113.3(3)
C(21)-C(20)-C(25)	115.8(3)	C(31)-C(29)-C(30)	109.6(3)
C(21)-C(20)-B(1)	123.4(3)	C(23)-C(29)-C(30)	110.5(3)
C(25)-C(20)-B(1)	120.6(3)	C(33)-C(32)-C(25)	110.9(3)
C(22)-C(21)-C(20)	121.8(3)	C(33)-C(32)-C(34)	110.1(3)
C(22)-C(21)-C(26)	114.8(3)	C(25)-C(32)-C(34)	111.7(3)
C(20)-C(21)-C(26)	123.2(3)		

Crystal structure of **5**

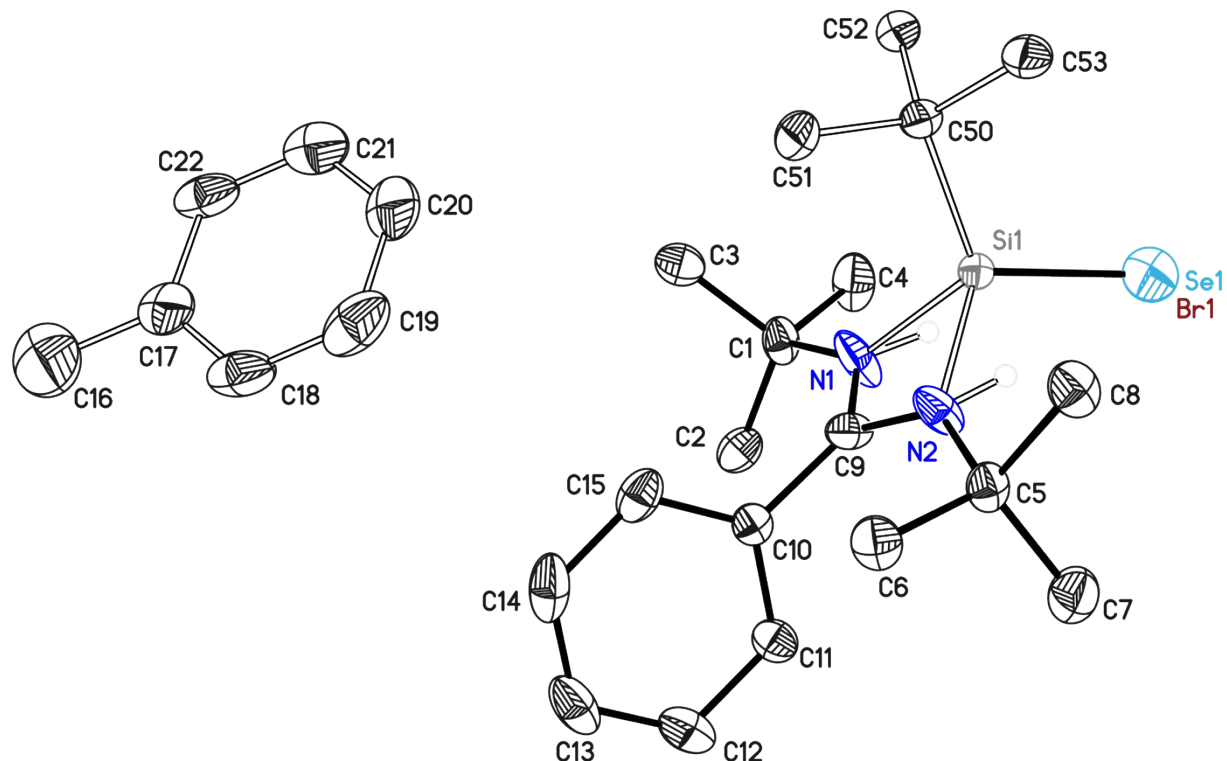


Figure S19: Crystal structure of **5**. The anisotropic displacement parameters are depicted at the 50% probability level. Hydrogen atoms are omitted for clarity.

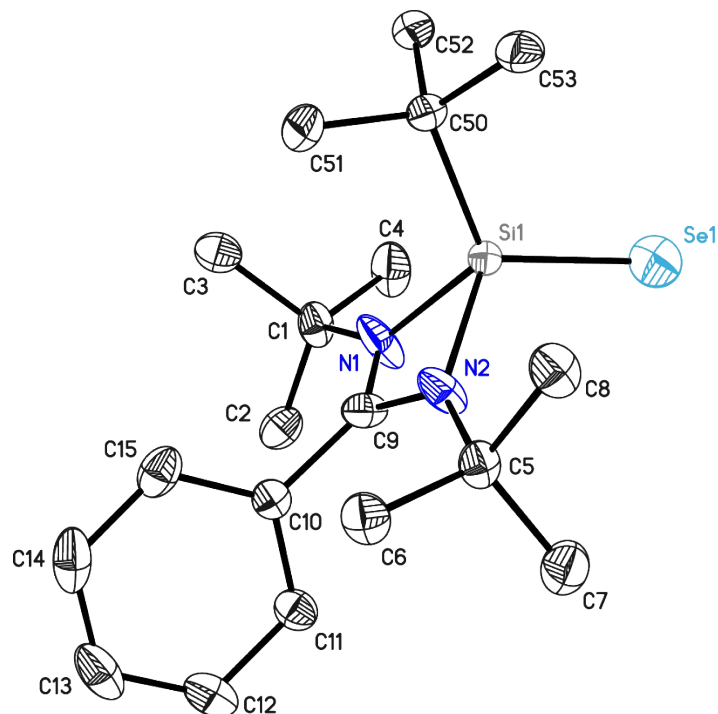


Figure S20: Excerpt of the crystal structure of **5**. Only compound **5** $\text{PhC}(\text{N}^t\text{Bu})_2\text{Si}(^t\text{Bu})=\text{Se}$ is shown. The anisotropic displacement parameters are depicted at the 50% probability level. Hydrogen atoms are omitted for clarity.

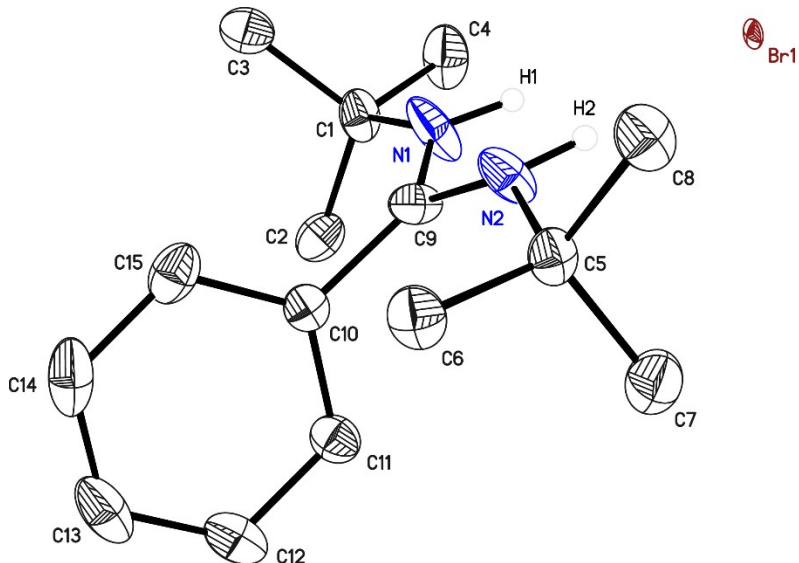


Figure S21: Excerpt of the crystal structure of **5**. Only $\text{PhC}(\text{NH}^t\text{Bu})_2\text{Br}$ is shown. The anisotropic displacement parameters are depicted at the 50% probability level. Hydrogen atoms except for H1 and H2 are omitted for clarity.

Two compounds, $\text{PhC}(\text{N}^t\text{Bu})_2\text{Si}(^t\text{Bu})=\text{Se}$ (**5**) and $\text{PhC}(\text{NH}^t\text{Bu})_2\text{Br}$, cocrystallized with one toluene molecule. $\text{PhC}(\text{N}^t\text{Bu})_2\text{Si}(^t\text{Bu})=\text{Se}$ (**5**) and $\text{PhC}(\text{NH}^t\text{Bu})_2\text{Br}$ are disordered about a two-fold axis, while the toluene molecule is disordered about an inversion centre. They were refined with distance restraints and restraints for the anisotropic displacement parameters.

Table S6: Bond lengths [Å] and angles [°] for **5**

C(1)-N(1)	1.4893(18)	N(1)-C(1)-C(4)	105.25(12)
C(1)-C(2)	1.521(2)	C(2)-C(1)-C(4)	109.16(14)
C(1)-C(3)	1.523(2)	C(3)-C(1)-C(4)	109.69(13)
C(1)-C(4)	1.534(2)	H(1)-N(1)-C(9)	117.3(19)
N(1)-H(1)	0.867(17)	H(1)-N(1)-C(1)	109.2(19)
N(1)-C(9)	1.3270(19)	C(9)-N(1)-C(1)	131.56(12)
N(1)-Si(1)	1.8990(15)	C(9)-N(1)-Si(1)	86.05(9)
Se(1)-Si(1)	2.1394(17)	C(1)-N(1)-Si(1)	139.18(11)
Si(1)-N(2)	1.8367(15)	N(2)-Si(1)-C(50)	113.96(10)
Si(1)-C(50)	1.899(3)	N(2)-Si(1)-N(1)	72.24(6)
Si(1)-C(9)	2.2406(16)	C(50)-Si(1)-N(1)	115.06(11)
C(50)-C(51)	1.538(4)	N(2)-Si(1)-Se(1)	114.49(7)
C(50)-C(52)	1.542(4)	C(50)-Si(1)-Se(1)	118.12(10)
C(50)-C(53)	1.547(4)	N(1)-Si(1)-Se(1)	114.65(8)
N(2)-H(2)	0.870(17)	N(2)-Si(1)-C(9)	36.41(5)
N(2)-C(9)	1.3305(18)	C(50)-Si(1)-C(9)	116.83(10)
N(2)-C(5)	1.4861(18)	N(1)-Si(1)-C(9)	36.22(5)
C(5)-C(7)	1.527(2)	Se(1)-Si(1)-C(9)	125.04(6)
C(5)-C(8)	1.528(2)	C(51)-C(50)-C(52)	109.5(2)
C(5)-C(6)	1.529(2)	C(51)-C(50)-C(53)	109.2(3)
C(9)-C(10)	1.4831(19)	C(52)-C(50)-C(53)	107.0(2)
C(10)-C(11)	1.390(2)	C(51)-C(50)-Si(1)	111.4(2)
C(10)-C(15)	1.391(2)	C(52)-C(50)-Si(1)	109.9(2)
C(11)-C(12)	1.391(2)	C(53)-C(50)-Si(1)	109.76(18)
C(12)-C(13)	1.384(3)	H(2)-N(2)-C(9)	114(2)
C(13)-C(14)	1.376(3)	H(2)-N(2)-C(5)	105(2)
C(14)-C(15)	1.394(2)	C(9)-N(2)-C(5)	132.02(12)
C(16)-C(17)	1.503(11)	C(9)-N(2)-Si(1)	88.55(9)
C(17)-C(18)	1.378(8)	C(5)-N(2)-Si(1)	139.33(10)
C(17)-C(22)	1.402(7)	N(2)-C(5)-C(7)	108.91(12)
C(18)-C(19)	1.383(7)	N(2)-C(5)-C(8)	104.46(11)
C(19)-C(20)	1.376(9)	C(7)-C(5)-C(8)	109.98(12)
C(20)-C(21)	1.369(9)	N(2)-C(5)-C(6)	113.42(12)
C(21)-C(22)	1.368(7)	C(7)-C(5)-C(6)	111.14(13)
		C(8)-C(5)-C(6)	108.70(12)
N(1)-C(1)-C(2)	112.40(12)	N(1)-C(9)-N(2)	111.96(13)
N(1)-C(1)-C(3)	109.84(13)	N(1)-C(9)-C(10)	125.26(12)
C(2)-C(1)-C(3)	110.37(12)	N(2)-C(9)-C(10)	122.76(12)

N(1)-C(9)-Si(1)	57.73(8)	C(10)-C(15)-C(14)	119.40(15)
N(2)-C(9)-Si(1)	55.03(7)	C(18)-C(17)-C(22)	117.6(4)
C(10)-C(9)-Si(1)	169.90(11)	C(18)-C(17)-C(16)	122.0(6)
C(11)-C(10)-C(15)	120.22(13)	C(22)-C(17)-C(16)	120.4(6)
C(11)-C(10)-C(9)	119.48(13)	C(17)-C(18)-C(19)	122.5(6)
C(15)-C(10)-C(9)	120.25(13)	C(20)-C(19)-C(18)	118.5(6)
C(10)-C(11)-C(12)	119.68(14)	C(21)-C(20)-C(19)	120.1(7)
C(13)-C(12)-C(11)	120.10(15)	C(22)-C(21)-C(20)	121.3(6)
C(14)-C(13)-C(12)	120.22(15)	C(21)-C(22)-C(17)	119.9(5)
C(13)-C(14)-C(15)	120.39(15)		

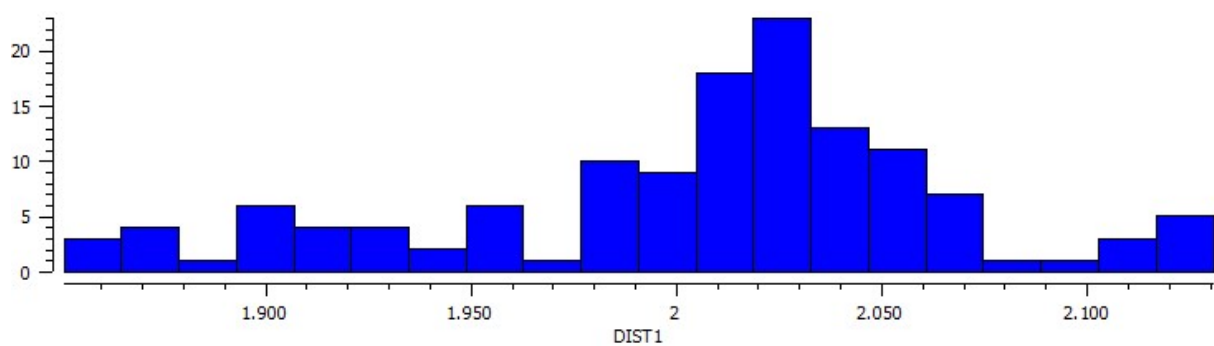


Figure S22: Histogram of all Si-B single bond lengths for structures containing a trivalent boron atom deposited in the CSD (version 5.43).^[7]

Computational Details:

All geometry optimizations were carried out with Gaussian09⁸ utilizing the Perdew–Burke–Ernzerhof exchange-correlation functional PBE.⁹ Unrestricted spin calculations were carried out for compounds with unpaired electrons. A def2-TZVPP basis set with a triple ζ -quality, augmented with two sets of polarization functions, was used for the geometry optimization.¹⁰ All stationary points were characterized on the potential energy hypersurface by vibrational analysis as minima (all real frequencies). Single point calculations were performed on the optimized geometries using the meta-GGA exchange functional M06-2X^[11] with the basis set having triple ζ -quality, augmented with two sets of polarization functions (def2-TZVPP). Natural Bond Orbital (NBO version 3.1)¹² analyses were performed at the M06-2X/def2-TZVPP//PBE/def2-TZVPP level of theory. Topological analysis of electron density based on QTAIM method¹³ was carried out using the AIMALL program package.¹⁴ The wave functions for the QTAIM analysis were generated using the Gaussian09 program at the M062X/def2-TZVPP//PBE/def2-TZVPP level of theory.

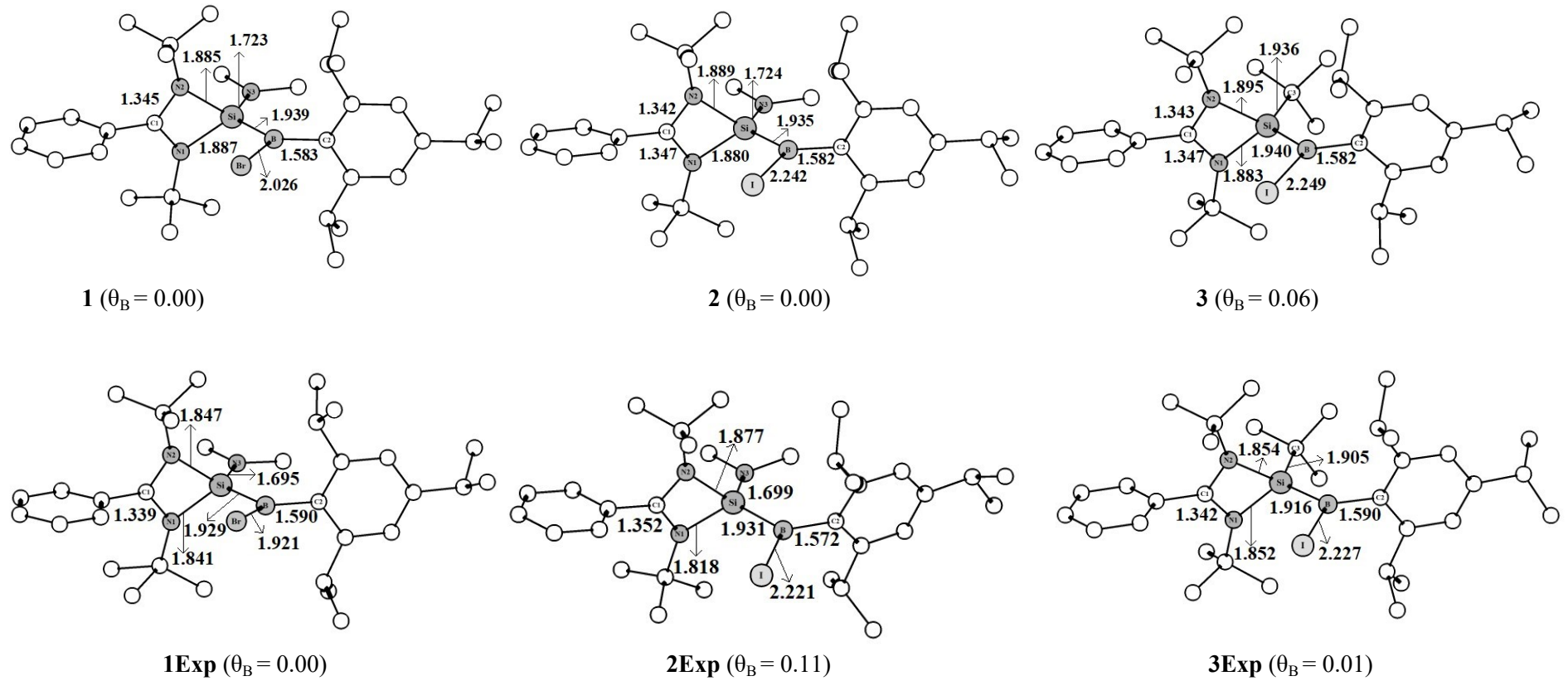


Figure S23: Optimized geometries of silicon-boron radical compounds **1-3** at the PBPBE/def2-TZVPP level of theory; θ_B gives the pyramidalisation angle around B (calculated as 360-sum of angles around B centre); Corresponding bond lengths in the experimental geometry given below in parenthesis

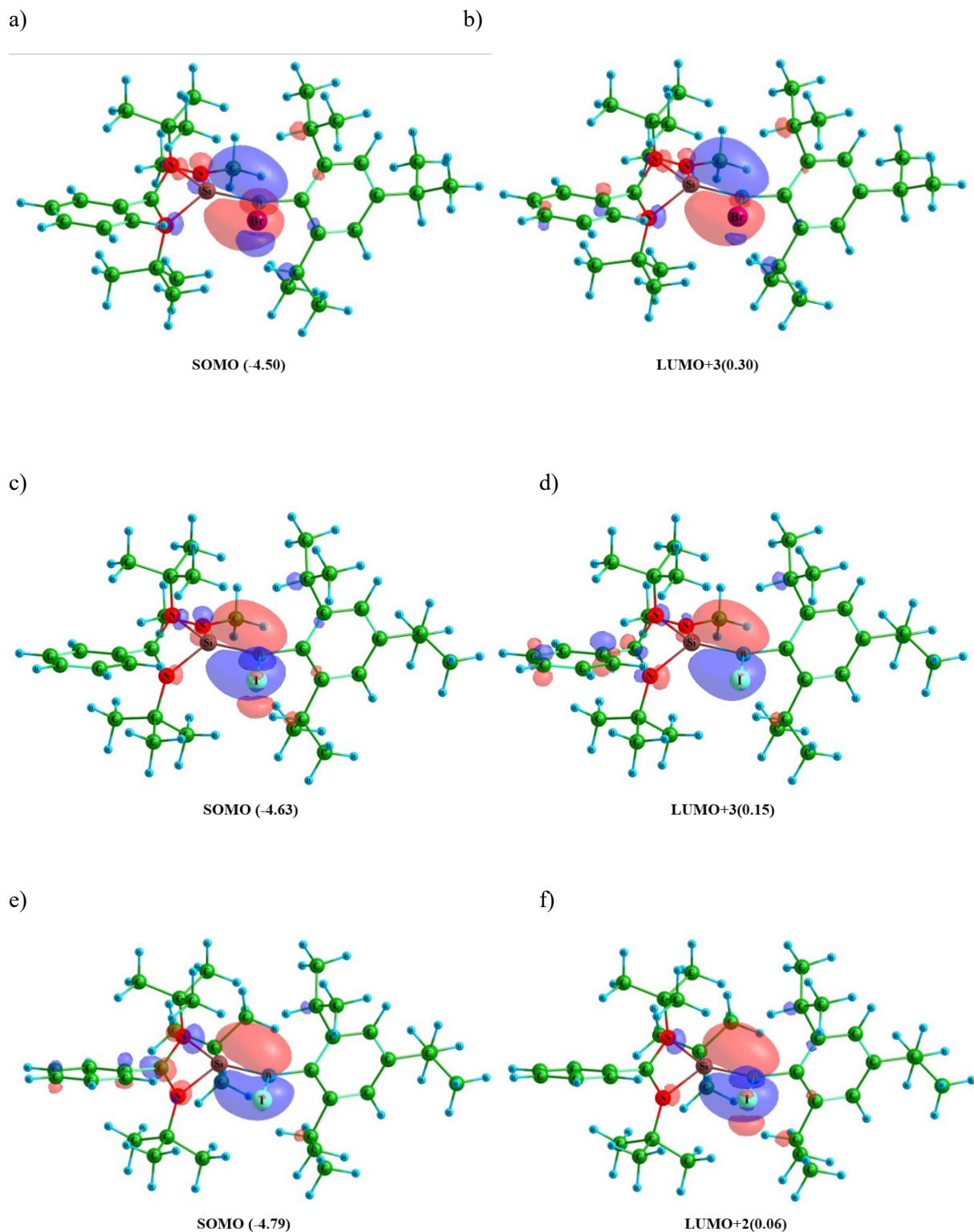


Figure S24: Selected frontier molecular orbitals of compounds **1-3** M062X/def2-TZVPP//PBPBE/def2-TZVPP level of theory; a), c) and e) depict the SOMO of compounds **1, 2, 3** respectively; b), d) and f) depict the corresponding unoccupied beta molecular orbitals of **1, 2, 3** respectively; Eigenvalue given in parenthesis; Isosurface value 0.05.

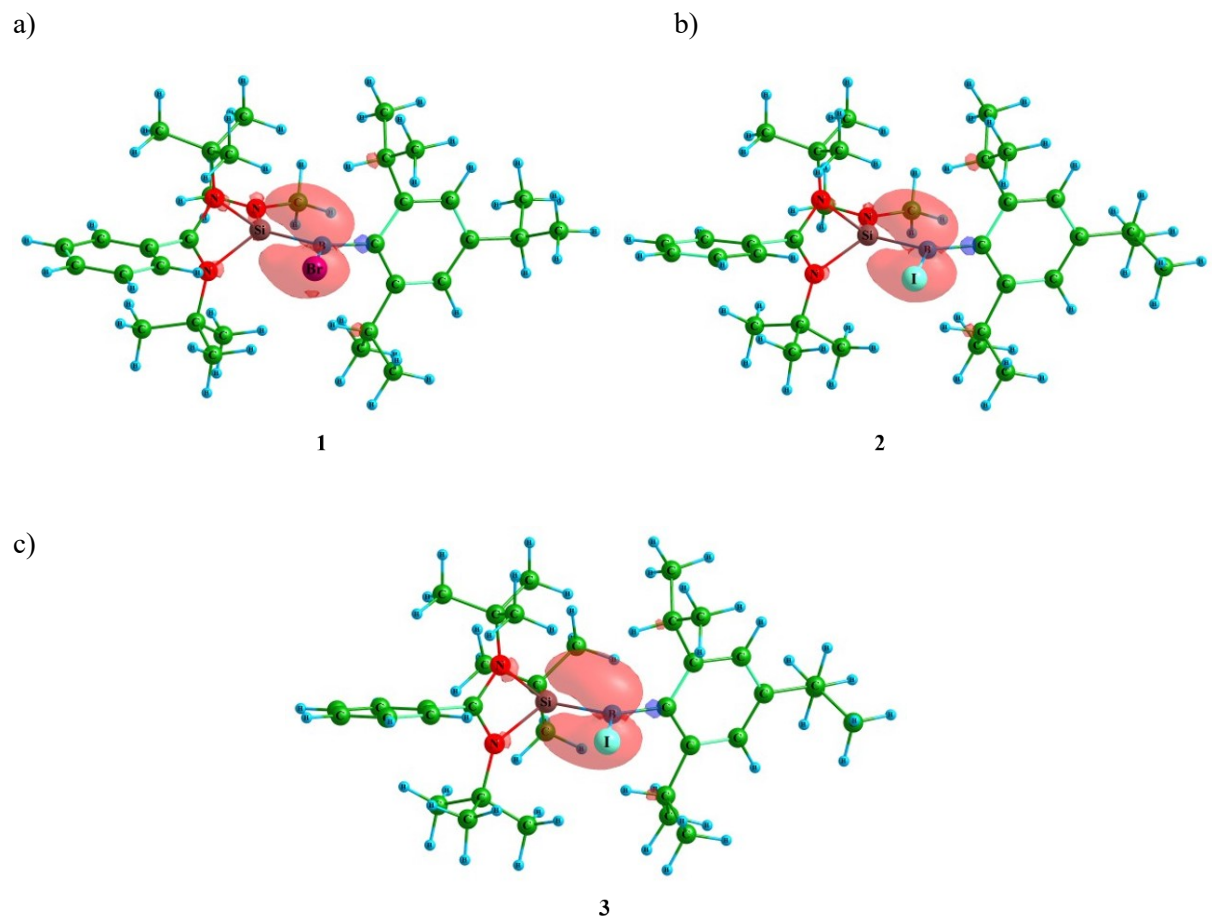
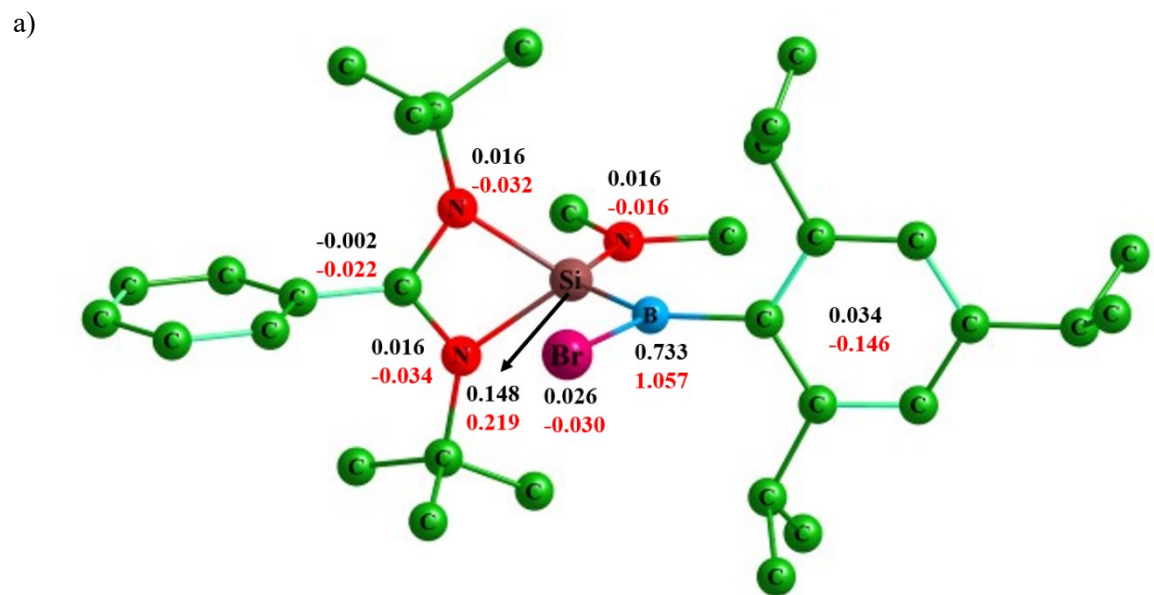
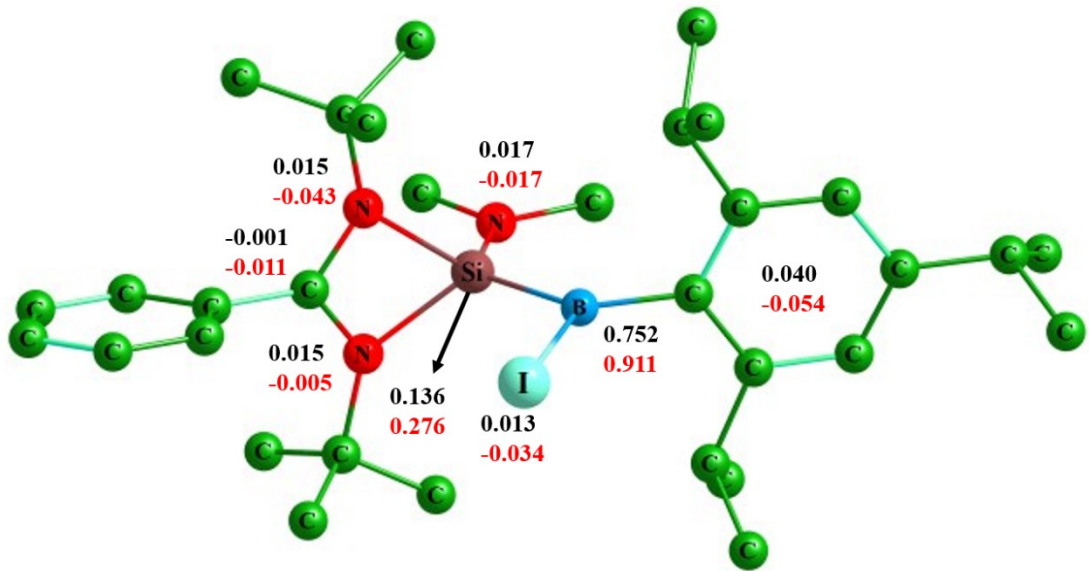


Figure S25: Spin density plots of compounds **1** - (a), **2** - (b) and **3** - (c) calculated at M062X/def2-TZVPP//PBE/def2-TZVPP level of theory; Isosurface value 0.0045.



b)



c)

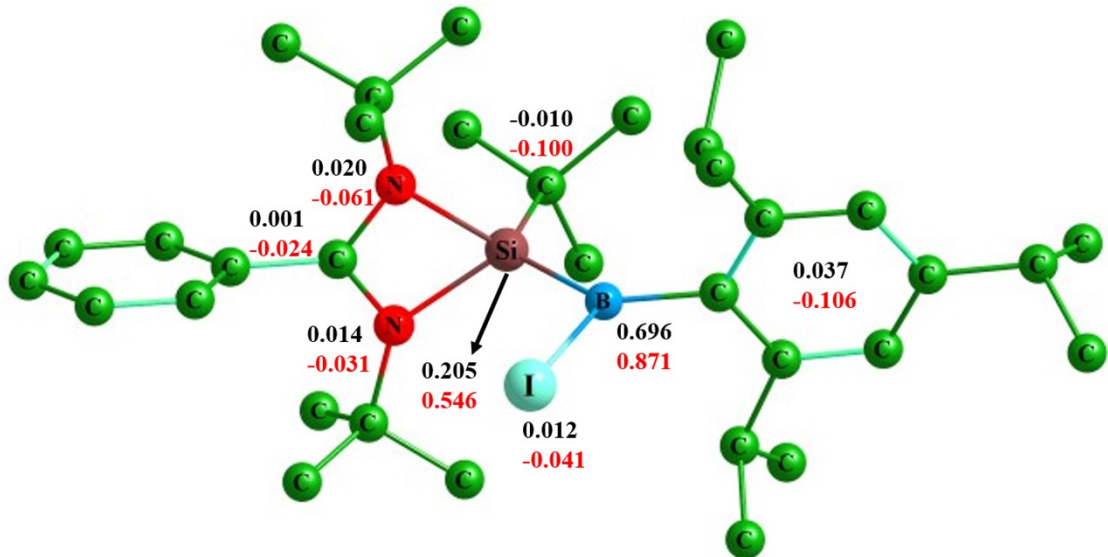


Figure S26: Natural spin density (black) and Mulliken spin density (red) of selected centres/groups in compounds 1 - (a), 2 - (b) and 3 - (c) calculated at the M062X/def2-TZVPP//PBE/def2-TZVPP level of theory; H atoms have been omitted for clarity.

Table S7: Natural charge (q), Wiberg bond indices (WBI) and bond orbital occupancy (BO) for selected centres/bonds from NPA and NBO analysis of compounds **1–3** at the M062X/def2-TZVPP//PBE/def2-TZVPP level of theory.

Compound	Centre	q	Bond	WBI	BO
1	Si	1.86	Si-B	1.07	0.97 (42.78%Si; 57.22%B)
	B	-0.29	B-Br	0.96	0.99
	Br	-0.23	Si-N1	0.41	0.81
	N1	-0.73	Si-N2	0.42	0.97
	N2	-0.74	N1-C1	1.39	0.99
	C1	0.54	N2-C1	1.39	0.99
					0.99
	N3	-0.91	B-C2	0.89	0.98
	C2	-0.38	Si-N3	0.66	0.98
			LP(1)B		0.75 (99.75%p)
			LP(1)N1		0.79 (99.78%p)
			LP(1)N3		0.91 (99.95%p)
			LP(1)Br		0.99 (25.62%p; 74.37%s)
			LP(2)Br		0.99 (99.99%p)
			LP(3)Br		0.97 (99.41%p)
2	Si	1.86	Si-B	1.08	0.97 (43.13%Si; 56.87%B)
	B	-0.33	B-I	0.98	0.98
	I	-0.17	Si-N1	0.42	0.97
	N1	-0.74	Si-N2	0.41	0.97
	N2	-0.73	N1-C1	1.38	0.99
	C1	0.55	N2-C1	1.40	0.99
					0.98
	N3	-0.91	B-C2	0.88	0.98
	C2	-0.41	Si-N3	0.65	0.98
			LP(1)B		0.76 (99.79%p)
			LP(1)N1		0.80 (99.70%p)
			LP(1)N3		0.91 (99.87%p)
			LP(1)I		0.99 (21.67%p; 78.32%s)
			LP(2)I		0.99 (99.82%p)
			LP(3)I		0.97 (99.40%p)
3	Si	1.79	Si-B	1.09	0.97 (41.40%Si; 58.60%B)
	B	-0.30	B-I	0.97	0.98
	I	-0.17	Si-N1	0.40	0.97
	N1	-0.76	Si-N2	0.37	0.97
	N2	-0.75	N1-C1	1.38	0.99
	C1	0.54	N2-C1	1.40	0.99
					0.98
	C3	-0.54	B-C2	0.87	0.98
	C2	-0.43	Si-C3	0.65	0.96
			LP(1)B		0.71 (99.76%p)
			LP(1)N1		0.80 (99.82%p)
			LP(1)I		0.99 (22.54%p; 77.45%s)
			LP(2)I		0.98 (99.91%p)
			LP(3)I		0.97 (98.95%p)

Table S8: Selected second-order interactions as given in the NBO analysis of compounds **1-3** at the M062X/def2-TZVPP//PBE/def2-TZVPP level of theory; Energy given in kcal mol⁻¹.

Compound	Donor orbital	Acceptor orbital	Energy
1	LP(1)B	BD*(1)Si-N1	14.43
		BD*(1)Si-N2	13.70
		BD*(1)C2-C _{adj}	5.09
		BD*(1)C2-C _{adj*}	5.08
		BD*(1)C _{iso} -H	1.67
		BD*(1)C _{iso*} -H	1.58
	LP(1)N3	BD*(1)Si-N1	10.5
		BD*(1)Si-N2	10.1
2	LP(1)B	BD*(1)Si-N1	11.25
		BD*(1)Si-N2	16.27
		BD*(1)C2-C _{adj}	5.49
		BD*(1)C2-C _{adj*}	5.50
		BD*(1)C _{iso} -H	1.56
		BD*(1)C _{iso*} -H	1.64
	LP(1)N3	BD*(1)Si-N1	9.86
		BD*(1)Si-N2	10.66
3	LP(1)B	BD*(1)Si-N1	11.60
		BD*(1)Si-N2	19.11
		BD*(1)C2-C _{adj}	5.18
		BD*(1)C2-C _{adj*}	5.38
		BD*(1)C _{iso} -H	1.29
		BD*(1)C _{iso*} -H	0.99

Table S9: Topological parameters of the electron density at the bond of **1-3** calculated at the M062X/def2-TZVPP//PBEPBE/def2-TZVPP level of theory; Electron density $\rho(r)$, Laplacian of electron density $\nabla^2\rho(r)$, potential energy density $V(r)$, kinetic energy density $G(r)$ and total energy density $H(r)$ are given in atomic units.

Compound	Bond/Ring	$\rho(r)$	$\nabla^2\rho(r)$	ϵ	$V(r)$	$G(r)$	$H(r)$
1	Si-B	0.1229	-0.0758	0.35	-0.1666	0.0738	0.1120
	B-Br	0.1000	-0.0757	0.11	-0.1508	0.0660	0.1040
	Si-N1	0.0954	0.2857	0.07	-0.1592	0.1153	-0.0275
	Si-N2	0.0958	0.2884	0.07	-0.1601	0.1161	-0.0281
	N1-C1	0.3401	-1.090	0.16	-0.7096	0.2186	0.7630
	N2-C1	0.3397	-1.0874	0.16	-0.7062	0.2172	0.7610
	B-C2	0.1778	-0.1841	0.03	-0.3350	0.1445	0.2370
	Si-N3	0.1319	0.5810	0.27	-0.2660	0.2056	-0.0849
2	Si-B	0.1229	-0.0677	0.32	-0.1682	0.0757	0.1090
	B-I	0.0865	-0.0907	0.02	-0.0746	0.0260	0.0713
	Si-N1	0.0967	0.2920	0.06	-0.1622	0.1176	-0.0284
	Si-N2	0.0951	0.2833	0.07	-0.1583	0.1146	-0.0271
	N1-C1	0.3386	-1.0821	0.16	-0.6964	0.2129	0.7540
	N2-C1	0.3414	-1.0971	0.16	-0.7232	0.2245	0.7730
	B-C2	0.1778	-0.1831	0.02	-0.3356	0.1449	0.2360
	Si-N3	0.1315	0.5776	0.26	-0.2647	0.2045	-0.0843
3	Si-B	0.1213	-0.0495	0.30	-0.1678	0.0774	0.1020
	B-I	0.0856	-0.0883	0.04	-0.0722	0.0251	0.0692
	Si-N1	0.0955	0.2932	0.04	-0.1599	0.1166	-0.0300
	Si-N2	0.0932	0.2781	0.04	-0.1540	0.1118	-0.0273
	N1-C1	0.3385	-1.0815	0.17	-0.7018	0.2157	0.7560
	N2-C1	0.3409	-1.0943	0.17	-0.7199	0.2232	0.7700
	B-C2	0.1787	-1.999	0.01	-0.3346	0.1423	0.2420
	Si-C3	0.1152	0.0946	0.03	-0.1709	0.0973	0.05000

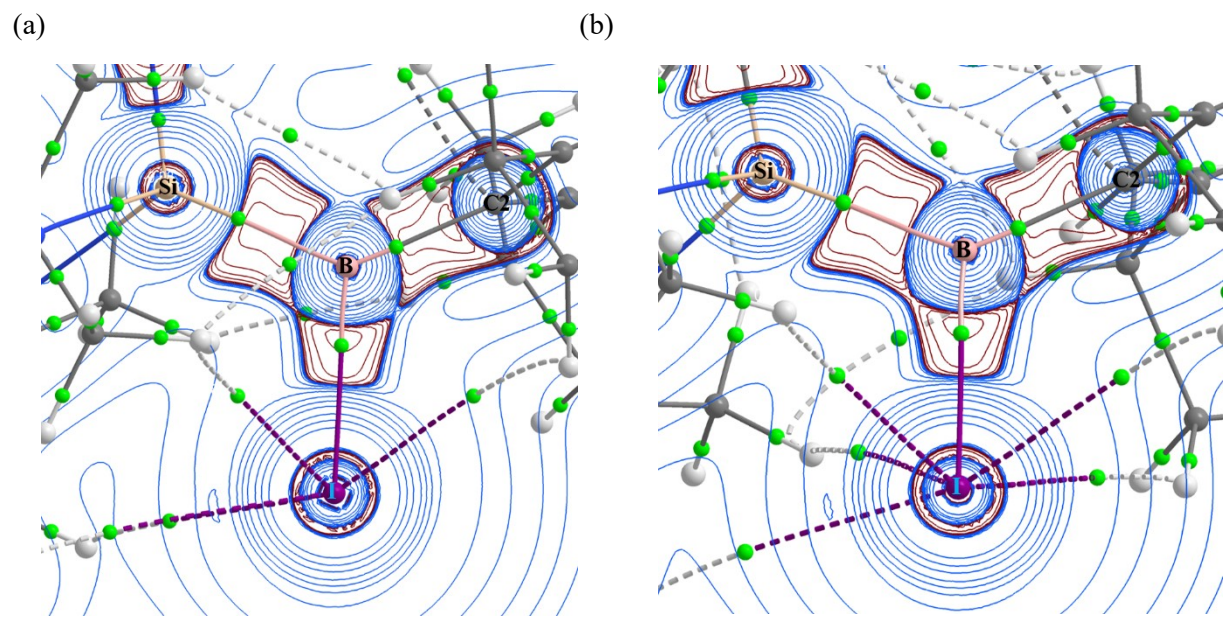


Figure S27: Laplacian of electron density plotted in the Si-B-C₂ plane of compounds **2** – (a) and **3** – (b).

Cyclic voltammetry

Cyclic voltammograms were recorded at room temperature in an N₂ glovebox using a Gamry Instruments Interface 1000B potentiostat and the Gamry Framework software. A three-electrode setup was applied using a glassy carbon disc as working electrode (ALS, 1.6 mm diameter), a platinum wire as auxiliary and a silver wire in a sample holder filled with electrolyte as pseudo-reference. Prior to use, the working disc electrode was polished with 0.05 µm alumina paste and the wires were sanded, and subsequently all electrodes were sonicated, rinsed with high purity deionized water and dried with a paper towel. The potentials were referenced against ferrocene, which was added to the analyte solution after the measurements. Tetrabutylammonium hexafluorophosphate was dried at 120 °C for 48 hours and used as conducting salt in acetonitrile. Dry and degassed acetonitrile was employed as solvent. The electrochemical measurements were evaluated with the Gamry EChem Analyst software.

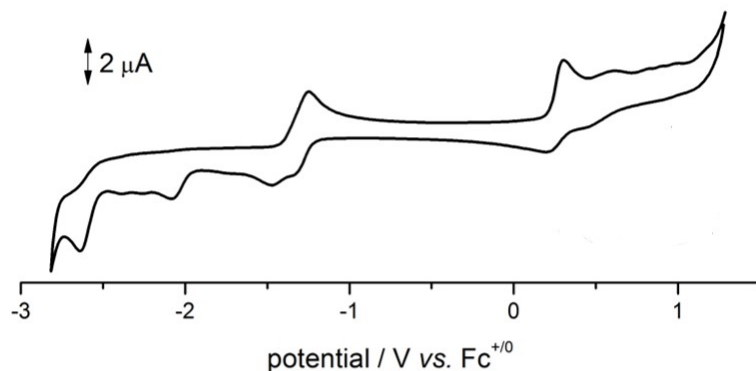


Figure S28: Full range cyclic voltammograms of 1mM solutions of **Si-B** radical in MeCN (0.1 M NBu_4PF_6) under inert conditions.

References

1. Bruker AXS Inc., in *Bruker Apex CCD, SAINT v8.30C* (Ed.: Bruker AXS Inst. Inc.), WI, USA, Madison, 2013.
2. L. Krause, R. Herbst-Irmer, G. M. Sheldrick, D. Stalke, *J. Appl. Crystallogr.* 2015, **48**, 3-10.
3. M. Sevvana, M. Ruf, I. Usón, G. M. Sheldrick, R. Herbst-Irmer, *Acta Crystallogr.* 2019, **D75**, 1040-1050.
4. G. M. Sheldrick, *Acta Crystallogr.* 2015, **A71**, 3-8.
5. G. M. Sheldrick, *Acta Crystallogr.* 2015, **C71**, 3-8.
6. C. B. Hübschle, G. M. Sheldrick, B. Dittrich, *J. Appl. Cryst.* 2011, **44**, 1281-1284.
7. C. R. Groom, I. J. Bruno, M. P. Lightfoot and S. C. Ward, *Acta Cryst.* 2016, **B72**, 171-179.
8. M. J.Frisch, G. W.Trucks, H. B.Schlegel, G. E.Scuseria, M. A.Robb, J. R.Cheeseman, G. Scalmani, V.Barone, B.Mennucci, G. A.Petersson, H.Nakatsuji, M.Caricato, X.Li, H. P.Hratchian, A. F.Izmaylov, J.Bloino, G.Zheng, J. L.Sonnenberg, M.Hada, M.Ehara, K.Toyota, R.Fukuda, J.Hasegawa, M.Ishida, T.Nakajima, Y.Honda, O.Kitao, H.Nakai, T.Vreven, J. A. Montgomery, Jr., J. E.Peralta, F.Ogliaro, M.Bearpark, J. J.Heyd, E.Brothers, K. N.Kudin, V. N.Staroverov, T.Keith, R.Kobayashi, J.Normand, K.Raghavachari, A.Rendell, J. C.Burant, S. S.Iyengar, J.Tomasi, M.Cossi, N.Regia, J. M.Millam, M.Klene, J. E.Knox, J. B.Cross, V.Bakken, C.Adamo, J.Jaramillo, R. Gomperts, R. E.Stratmann, O.Yazyev, A. J.Austin, R.Cammi, C.Pomelli, J. W. Ochterski, R. L.Martin, K.Morokuma, V. G.Zakrzewski, G. A. Voth, P.Salvador, J. J.Dannenberg, S.Dapprich, A. D. Daniels, O. Farkas, J. B. Foresman, J. V.Ortiz, J.Cioslowski and D. J.Fox, Gaussian, Inc., Wallingford CT, 2010
9. M. Ernzerhof, G. E. Scuseria *J. Chem. Phys.* 1999, **110**, 5029; b) J. P. Perdew, K. Burke, M. Ernzerhof *Phy. Rev. Lett.*, 1997, **78**, 1396.
10. F. Weigend, R. Ahlrichs, *Phys. Chem. Chem. Phys.* 2005, **7**, 3297-3305.
11. Y. Zhao and D. G. Truhlar, *Theor. Chem. Acc.* 2008, **120**, 215-241
12. E.Reed, L. A.Curtiss and F.Weinhold, *Chem. Rev.* 1988, **88**, 899–926; (b) NBO 3.1. E. D. Glendening, J. K. Badenhoop, A. E.Reed, J. E.Carpenter, J. A. Bohmann, C. M. Morales, C. R. Landis and F. Weinhold (Theoretical Chemistry Institute, University of Wisconsin, Madison, WI, 2013).
13. R. F. W. Bader, Atoms in Molecules. A Quantum Theory, Oxford University Press, Oxford, 1990; (b) C. F. Matta and R. J. Boyd, The Quantum Theory of Atoms in Molecules, Wiley-VCH, Weinheim, 2007.
14. T. A. Keith, AIMAll (Version 15.05.18), TK Gristmill Software, Overland Park, KS, USA, 2015 (aim.tkgristmill. com).